LUND UNIVERSITY

Perinatal Risk Factors for Morbidity and Mortality in Left Heart Anomalies

Fricke, Katrin

2024

Document Version:
Publisher's PDF, also known as Version of record

Link to publication

Citation for published version (APA):
Fricke, K. (2024). *Perinatal Risk Factors for Morbidity and Mortality in Left Heart Anomalies*. [Doctoral Thesis (compilation), Department of Clinical Sciences, Lund]. Lund University, Faculty of Medicine.

Total number of authors:
1

General rights
Unless other specific re-use rights are stated the following general rights apply:
Copyright and moral rights for the publications made accessible in the public portal are retained by the authors and/or other copyright owners and it is a condition of accessing publications that users recognise and abide by the legal requirements associated with these rights.
• Users may download and print one copy of any publication from the public portal for the purpose of private study or research.
• You may not further distribute the material or use it for any profit-making activity or commercial gain
• You may freely distribute the URL identifying the publication in the public portal

Read more about Creative commons licenses: https://creativecommons.org/licenses/

Take down policy
If you believe that this document breaches copyright please contact us providing details, and we will remove access to the work immediately and investigate your claim.

LUND UNIVERSITY

PO Box 117
221 00 Lund
+46 46-222 00 00

Perinatal Risk Factors for Morbidity and Mortality in Left Heart Anomalies

KATRIN FRICKE
DEPARTMENT OF EXPERIMENTAL MEDICAL SCIENCE | LUND UNIVERSITY

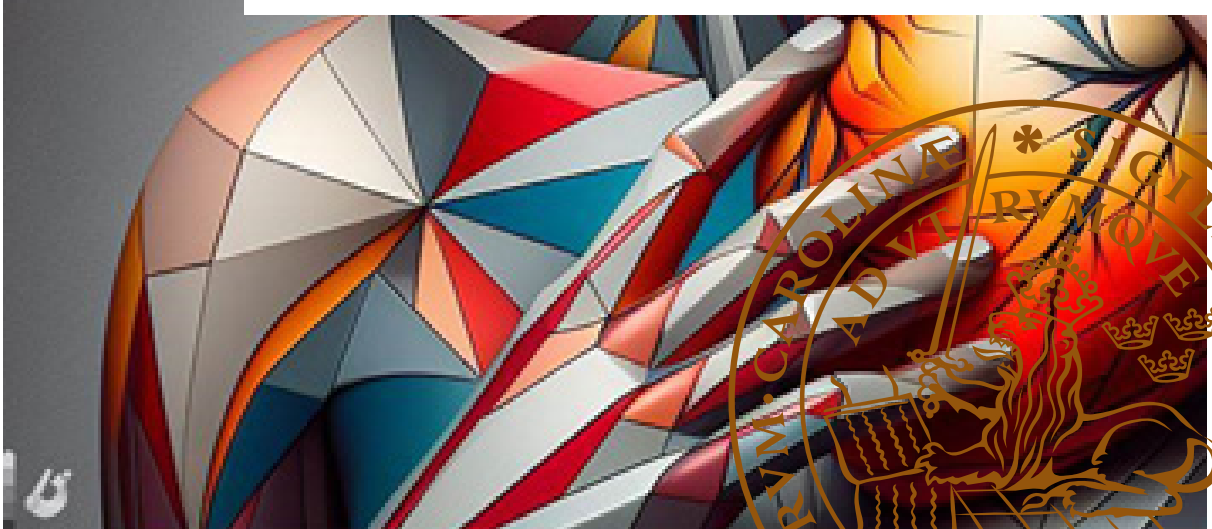

Perinatal Risk Factors for Morbidity and Mortality in Left Heart Anomalies

Perinatal Risk Factors for Morbidity and Mortality in Left Heart Anomalies

Katrin Fricke

LUND
UNIVERSITY

DOCTORAL DISSERTATION

For the degree of Doctor of Philosophy (PhD) at the Faculty of Medicine,

at Lund University to be publicly defended on February 16th at 09.00 in Belfragesalen, BMC, Lund, Sweden.

Faculty opponent
Professor John Simpson, Evelina London Children´s Hospital,
Guy´s and St Thomas´ NHS Foundation Trust, London, United Kingdom

Organization: LUND UNIVERSITY

Faculty of Medicine

Date of issue: 2024-02-16

Sponsoring organization: None

Document name: Doctoral thesis

Author: Katrin Fricke

Title: Perinatal risk factors for morbidity and mortality in left heart anomalies

Abstract

Background: Left heart obstructions include different stenotic lesions in the left ventricle and in the aorta, ranging from discrete to severe phenotypes requiring neonatal surgical or transcatheter interventions. The latter include hypoplastic left heart syndrome (HLHS) and critical aortic coarctation (CoA) with or without aortic arch hypoplasia. Severe left heart obstructions are associated with significant morbidity and mortality, especially if the diagnosis is not made early after birth before arterial duct closure. Therefore, fetal diagnosis is pivotal to plan delivery in a tertiary referral centre for pediatric cardiac surgery and to reduce morbidity and mortality. In some cases, left heart obstruction is suspected in utero, but cannot be confirmed or ruled out. This is particularly true for CoA, which can be detected prenatally by indirect signs such as ventricular or arterial dysproportion with smaller left heart structures. However, less than half of fetuses with ventricular dysproportion develop CoA.

Even when the diagnosis is made in time, neonates with CoA or HLHS may experience complications, highlighting the need for risk stratification and careful follow-up.

The aims of this thesis were to 1) improve the fetal diagnosis of suspected left heart obstructions, including CoA, 2) characterize aortic arch geometry and flow in neonates following CoA repair, and 3) identify morphological and surgical predictors of adverse outcome after stage I palliation of HLHS.

Methods and Results: In ***Study I***, we conducted a retrospective study of of 65 fetuses born between 2010 and 2018 with fetal suspicion of isolated CoA. Postnatal CoA could be accurately predicted by using the carotid-subclavian artery index or the aortic isthmus-to-duct ratio in the three-vessel trachea view together with the mitral-to-tricuspid valve ratio. In ***Study II*****,** we conducted a retrospective national study of 167 patients with HLHS and Norwood stage I palliation between 1999 and 2018. The anatomic HLHS subtype aortic atresia-mitral stenosis (AA-MS) and a globular left ventricle were independent risk factors for adverse outcome, particularly when a Blalock-Taussig shunt was used as part of their Norwood stage I palliation. ***Study III*** was a prospective study of 51 fetuses with suspected left heart obstructions (HLHS, critical aortic stenosis (cAS) and CoA) and controls. Fetal cardiac magnetic resonance imaging (CMR) of the descending aorta and umbilical vein could not aid to discriminate between fetuses with and without the need for neonatal cardiac intervention, but identified those with more severe reduction in blood flow through the left side of the heart. ***Study IV*** was a prospective study of 28 neonates with CoA repair in whom MRI was used to characterize aortic arch geometry and four-dimensional (4D) flow prior to discharge after CoA surgery. Patients who developed recurrent coarctation (re-CoA) within the first 12 months (4 out of 28) showed postoperative changes in aortic arch geometry and flow pattern compared to those without re-CoA.

Conclusions: This thesis may provide additional insights into the fetal diagnosis of severe left heart obstructions and in the understanding of the clinical implications of certain anatomic and flow phenotypes after neonatal surgery.

Key words: hypoplastic left heart syndrome, coarctation of the aorta, recurrent coarctation, major adverse events, fetal echocardiography, fetal cardiac magnetic resonance imaging

Classification system and/or index terms: none

Supplementary bibliographical information: none

Language: English

ISSN: 1652-8220

ISBN: 978-91-8021-516-9

Number of pages: 86

I, the undersigned, being the copyright owner of the abstract of the above-mentioned dissertation, hereby grant to all reference sources permission to publish and disseminate the abstract of the above-mentioned dissertation.

Signature

Date 2024-01-03

Perinatal Risk Factors for Morbidity and Mortality in Left Heart Anomalies

Katrin Fricke

LUND
UNIVERSITY

Supervisor:
Petru Liuba, Associate Professor, University Lecturer

Co-supervisors:
Erik Hedström, Associate Professor
Katarina Hanséus, Associate Professor
Constance Weismann, Associate Professor
Pia Sjöberg MD, PhD

Coverphoto generated by Bing image creator

Dissertational Thesis - Copyright © 2024 Katrin Fricke
Paper I © The Authors 2020
Paper II © The Authors 2021
Paper III © The Authors 2023
Paper IV © The Authors (Manuscript unpublished)

Lund University
Faculty of Medicine
Department of Experimental Medical Science

ISBN 978-91-8021-516-9
ISSN 1652-8220

Printed in Sweden by Media-Tryck, Lund University
Lund 2024

Media-Tryck is a Nordic Swan Ecolabel certified provider of printed material. Read more about our environmental work at www.mediatryck.lu.se
MADE IN SWEDEN

“Questions you cannot answer are usually far better for you than answers you cannot question.”

Yuval Noah Harari
21 Lessons for the 21st Century

Table of Contents

List of Papers

Papers included in this thesis

Paper I

Fricke K, Liuba P, Weismann CG. Fetal Echocardiographic Dimension Indices: Important Predictors of Postnatal Coarctation. Pediatric Cardiology. 2021 Mar;42(3):517-525. doi: 10.1007/s00246-020-02509-6.

Paper II

Fricke K, Mellander M, Hanséus K, Tran PK, Synnergren M, Johansson Ramgren J, Rydberg A, Sunnegårdh J, Dalén M, Sjöberg G, Weismann CG, Liuba P. Impact of Left Ventricular Morphology on Adverse Outcomes Following Stage 1 Palliation for Hypoplastic Left Heart Syndrome: 20 Years of National Data From Sweden. Journal of the American Heart Association. 2022 Apr 5;11(7):e022929. doi: 10.1161/JAHA.121.022929.

Paper III

Fricke K, Ryd D, Weismann CG, Hanséus K, Hedström E, Liuba P. Fetal cardiac magnetic resonance imaging of the descending aorta in suspected left-sided cardiac obstructions. Front Cardiovasc Med. 2023 Dec 1;10:1285391. doi: 10.3389/fcvm.2023.1285391. PMID: 38107261; PMCID: PMC10725198.

Paper IV

Fricke K, Christierson L, Heiberg E, Sjöberg P, Hedström E, Weismann CG, Töger J, Liuba P. Three-dimensional Arch Geometry and Blood Flow in Neonates After Surgical Repair for Aortic Coarctation (manuscript).

Papers not included in this thesis

Mockenhaupt FP, Bedu-Addo G, von Gaertner C, Boyé R, **Fricke K**, Hannibal I, Karakaya F, Schaller M, Ulmen U, Acquah PA, Dietz E, Eggelte TA, Bienzle U. Detection an clinical manifestation of placental malaria in southern Ghana. Malar J 2006 Dec 13; 5:119.doi:10.1186/1475-2875-5-119.PMID:17166266; PMCID: PMC1716171.

Ryd D, **Fricke K**, Bhat M, Arheden H, Liuba P, Hedström E. Utility of Fetal Cardiovascular Magnetic Resonance for Prenatal Diagnosis of Complex Congenital Heart Defects. JAMA Netw Open. 2021 Mar 1;4(3):e213538. doi: 10.1001/jamanetworkopen.2021.3538. Erratum in: JAMA Netw Open. 2021 Apr 1;4(4):e2111261. Erratum in: JAMA Netw Open. 2022 Mar 1;5(3):e225825. PMID: 33779747; PMCID: PMC8008290.

Fricke K, Bhat M, Avdikos V, Asp A, Brodszki J, Thurn L. Fler medfödda hjärtfel upptäcks med utökad screening i tre steg [High prenatal detection rates of complex congenital heart defects (CHD)]. Lakartidningen. 2021 Nov 17;118:21091. Swedish. PMID: 35080769.

Sjöberg P, Hedström E, **Fricke K**, Frieberg P, Weismann CG, Liuba P, Carlsson M, Töger J. Comparison of 2D and 4D Flow MRI in Neonates Without General Anesthesia. J Magn Reson Imaging. 2023 Jan;57(1):71-82. doi: 10.1002/jmri.28303. Epub 2022 Jun 21. PMID: 35726779; PMCID: PMC10084310.

Abbreviations

AA-MA	Aortic atresia-mitral atresia
AA-MS	Aortic atresia-mitral stenosis
AS-MS	Aortic stenosis- mitral stenosis
AAo	Ascending aorta
AUC	Area under the curve
BTs	modified Blalock-Taussig shunt
cAS	Critical aortic stenosis
CHD	Congenital heart defect
CoA	Coarctation of the aorta
CSAI	Carotid-subclavian artery index
CT	Computed tomography
DAo	Descending aorta
DUS	Doppler ultrasound
EFE	Endocardial fibroelastosis
Fetal CMR	Fetal cardiac magnetic resonance imaging
FGR	Fetal growth restriction
Glob-LV	Globular left ventricle
HLHS	Hypoplastic left heart syndrome
IAS	Intact atrial septum
ICC	Intraclass correlation coefficient
$I/D_{(3VT)}$	Isthmus-to-duct ratio in the three-vessel trachea view
I/D_{3VT} x MV/TV	Product of I/D with the mitral-to-tricuspid valve ratio
IS-I	Interstage I
IQR	Interquartile range
LPW	Low preoperative weight
L-SVC	Persistent left superior vena cava
MAE	Major adverse events
MRI	Magnetic resonance imaging

n	Number of patients for a given variable
N	Total number of patients
RAS	Restrictive atrial septum
ROC	Receiver operating characteristic curve
S1P	Norwood stage I palliation
SVR	Single Ventricle Reconstruction
TCPC	Total cavopulmonary connection
TR	Tricuspid regurgitation
UV	Umbilical vein
VSD	Ventricular septal defect
VTI	Velocity time integral
3VT	Three-vessel trachea view

Populärvetenskaplig sammanfattning

Vänstersidiga hjärtobstruktioner inkluderar olika fenotyper som innefattar allt från en förträngning i aortabåge (aortakoarktation eller CoA), borderline vänstersidiga hjärtstrukturer, till en uttalad underutveckling av vänster hjärthalvan, som kallas för hypoplastiskt vänsterkammarsyndrom eller HLHS.

Patienter med allvarliga vänstersidiga utflödesobstruktioner löper stor risk för sjuklighet och dödlighet. Vid utebliven diagnos tidigt efter födelsen kan slutningen av en fosterförbindelse kallad ductus arteriosus leda till snabb klinisk försämring som kan kulminera med död inom timmar till dagar. Därför är en diagnos i god tid (främst under fosterlivet eller senast inom första levnadsveckan) av ytterst stor vikt.

CoA är ett av de vanligaste hjärtfelen och utgör ungefär 8-10% av alla medfödda hjärtfel. Diagnos av CoA under fosterlivet är mycket svårt, med låg andel upptäckta fall (20-30%), då tydlig förträngning oftast först utvecklas i nyföddhetsperioden när ductus stängs. Ett indirekt tecken på förekomst av CoA under fosterlivet är en storleksskillnad mellan vänster- och höger hjärthalva, med mindre vänstersidiga hjärtstrukturer. Intressant nog utvecklar enbart 50% av dessa foster CoA, vilket leder till överdiagnostik förknippad med onödig rädsla bland blivande föräldrar och onödigt bruk av hälsovårdens resurser. Trots tidsnära diagnos, med lyckad operation i nyföddhetsperioden, kan komplikationer uppstå. En av de vanligaste är en återkommande förträngning i aortabågen (re-CoA), som uppstår i 10-20% av fall som opereras i nyföddhetsperioden, detta oftast inom några månader efter genomgången CoA operation.

HLHS är extremvarianten av vänstersidiga utflödesobstruktioner, och utgör ungefär 50% av enkammarhjärtan. Vänsterhjärthalvan kan då inte pumpa blodet till kroppen. HLHS upptäcks lätt under fosterlivet, då man tydligt ser att vänsterkammaren är mycket litet eller saknas helt vid fosterundersökning. Det finns olika subtyper av HLHS gällande hur den underutvecklade vänstra kammaren och in-och utflödesklaffar (mitralis- och aortaklaff) ser ut och fungerar. Det misstänks att vissa av dessa subtyper skulle kunna vara förknippade med högre risk för komplikationer i nyföddhetsperioden eller senare i livet.

Syftet med denna avhandling var att förbättra prenatal diagnostik och utfall hos patienter med vänstersidiga obstruktioner.

Studie I var en retrospektiv studie, som syftade till att hitta faktorer som redan under fosterlivet kunde hjälpa förutsäga utveckling av CoA i nyföddhetsperioden. I denna studie inkluderades 65 foster med misstänkt CoA varav 22 (34%) utvecklade CoA i nyföddhetsperioden. Vi kunde identifiera två fostereko-baserade faktorer, som kunde förutspå CoA med hög precision. Detta skulle kunna hjälpa minska förekomsten av felaktig fetal diagnostisering av CoA (falskt positiv CoA) och leda till optimal användning av sjukhusresurser till nyfödda med bekräftad CoA.

Studie II var en retrospektiv nationell studie, som syftade till att identifiera risk-faktorer för kort och långtidssjuklighet och dödlighet relaterad till vänsterkammarens utseende, mitralis- och aortaklaff funktion (morfologi) och operationsmetod i nyföddhetsperioden. I denna studie fann vi att barn med HLHS varianterna med antingen 1) en stängd aorta- och öppen, men underutvecklad mitralisklaff (AA-MS) eller 2) med en tjock, kort och rundad (globulär) vänsterkammare, hade ökad sjuklighet och dödlighet, speciellt om dem opererades vid första operationssteg med en så kallad modifierad Blalock-Taussig (BT) shunt. Att ta hänsyn till dessa riskfaktorer skulle kunna minska dödlighet och sjuklighet.

Studie III var en prospektiv fosterstudie, som syftade till att förbättra den prenatala diagnostiken av vänstersidiga hjärtobstruktioner med tillägg av magnetkamera (foster-CMR) baserade flödesundersökningar i bukaortan och navelvenen till fostereko. I denna studie kunde vi inte skilja mellan foster med misstänkta vänstersidiga hjärtobstruktioner med och utan behov av operation i nyföddhetsperioden, men identifiera dessa med uttalat minskat flöde genom vänstra hjärthalvan. Detta skulle kunna hjälpa att identifiera foster med höggradiga utflödesobstruktioner, speciellt i sen graviditet, när ekofönstren oftast är dåliga.

Studie IV var en prospektiv studie, som inkluderade barn med CoA som behövde opereras i nyföddhetsperioden. Syftet med studien var att karakterisera båggeometrin och blodflöde i aortabågen efter CoA operation i nyföddhetsperioden och jämföra dessa mellan barn, som hade och inte hade återkomst av förträngning i aortabågen (re-CoA). I studien använde vi oss av nya MR metoder såsom 4D flöde och beräknade 3D vinklar av aortabågen. Fyra barn (14%) utvecklade re-CoA inom första levnadsåret och visade en annorlunda båggeometri och flödesmönster i aortabågen jämfört med de, som inte utvecklade re-CoA.

Sammanfattningsvis kunde vi visa att den prenatala diagnosen av allvarliga vänstersidiga hjärtobstruktioner kan förbättras med hjälp av fostereko och/eller foster-CMR markörer. Därtill hittade vi riskfaktorer som skulle kunna vara förknippade med allvarligt utfall hos nyfödda med HLHS eller CoA. Om dessa beaktas, så skulle detta kunna förbättra utfallet för dessa patientgrupper.

Introduction and background

Left heart obstructions involve a variety of phenotypes ranging from coarctation of the aorta (CoA) with or without aortic arch hypoplasia, borderline left heart structures with or without significant valvular stenosis, to hypoplastic left heart syndrome (HLHS) with a severely underdeveloped left ventricle (LV) and the need for univentricular palliation.

Prenatal diagnosis of left heart obstructions is essential to identify fetuses with severe lesions requiring neonatal intervention and facilitates optimal counselling, planning of delivery and perioperative care, thereby preparing expectant parents and reducing neonatal morbidity and mortality. Correct prenatal diagnosis can also reduce the proportion of false positive diagnoses, thereby avoiding unnecessary parental anxiety and overuse of healthcare resources.

Postoperative complications, including early re-intervention or even death, are still quite common. Identifying infants at risk for such complications is therefore important.

Coarctation of the aorta (CoA)

Background

Coarctation of the aorta is a common congenital heart defect (CHD), which accounts for approximately 8-10% of all CHDs [1]. CoA is defined as a narrowing of the aortic arch, usually at the insertion of the arterial duct in the isthmic region. However, more severe subtypes with a tubular hypoplasia of parts or the entire aortic arch may occur as well (*Figure 1*). CoA may present in isolation or in association with other types of CHDs. Commonly associated minor CHDs include ventricular septal defects (VSDs) or bicuspid aortic valve (BAV). CoA is difficult to predict prenatally because the final narrowing in the aortic arch is not apparent until the arterial duct closes. If the narrowing of the aortic arch is mild, the newborn is usually asymptomatic. Over time, collaterals can form and those affected may later present with arterial hypertension/a blood pressure gradient between arm and leg, headaches or a heart murmur. However, when critical narrowing occurs with ductal closure, there is an acute decrease in perfusion to the lower body and an increase in left

ventricular afterload, which can lead to serious conditions such as heart failure, shock or death.

Theoretically, neonatal pulse oximetry (POX) screening may help to identify neonates with critical left heart obstructions and duct-dependent systemic circulation due to right-left shunting at the ductal level with subsequent desaturation in the lower part of the body. In a recent nationwide Swedish study, only 12% of neonates with critical CoA were identified by POX screening and 28% by neonatal clinical examination, leaving 30% undiagnosed at discharge [2]. Therefore, a timely, preferably fetal diagnosis is essential to allow optimal planning of delivery and perinatal care to prevent unnecessary morbidity and mortality [3].

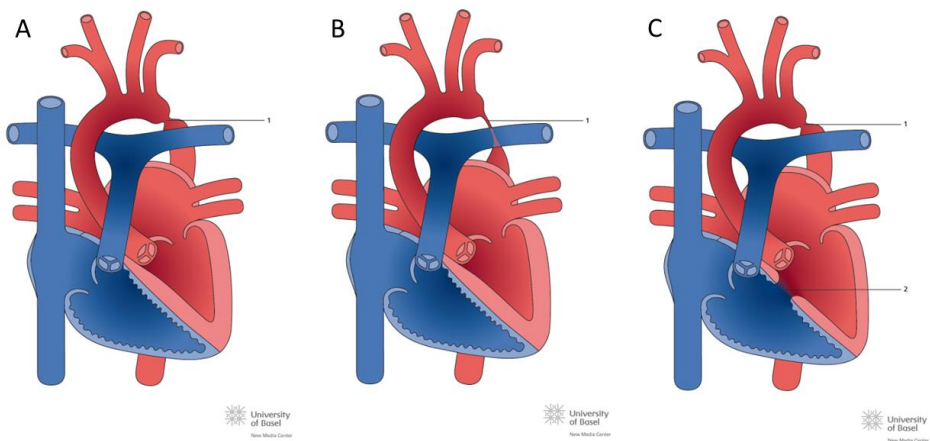

Figure 1: Subtypes of coarctation: A) Simple CoA with focal narrowing (1), B) Tubular hypoplasia of the aortic arch (1), C) CoA (1) with ventricular septal defect (2). *Illustration taken from Congenital Heart Disease (chd-diagrams.com)*

Fetal diagnosis of CoA

Despite intense research efforts and technological advances in fetal echocardiography, fetal diagnosis of CoA remains challenging with detection rates as low as 20-35% in some centres [4,5]. Improvements in fetal cardiac screening may increase fetal detection rates [5,6], but sometimes no obvious changes consistent with CoA are present in fetal life and may only occur after birth when the arterial duct closes. These cases cannot be detected prenatally.

The presence of fetal CoA is suspected, when a disproportion of the ventricles and great arteries with smaller left heart structures is noticed on the fetal echocardiogram (*Figure 2*). However, right ventricular dominance, a physiological finding in late gestation, as well as other cardiac conditions associated with reduced blood flow to the left side of the heart, may give the false impression of the presence of fetal CoA.

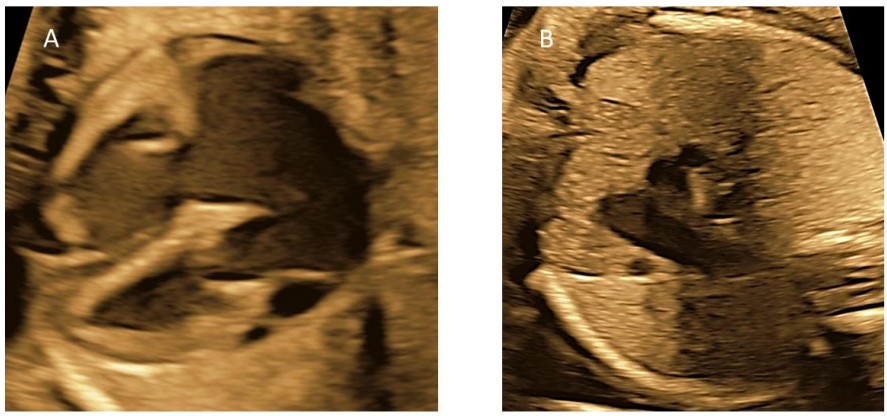

Figure 2: Disproportion of the ventricles and great arteries in a fetus at 27 weeks´ gestation with suspected coarctation. A) Four-chamber view showing ventricular disproportion with a smaller left ventricle and a dilated coronary sinus due to a persistent left superior vena cava (L-SVC). B) Three-vessel view demonstrating great artery disproportion with a smaller ascending aorta, as well as the presence of L-SVC.

To note, less than 50% of fetuses with a ventricular disproportion develop postpartum CoA, leading to high false positive detection rates associated with unnecessary parental anxiety and use of healthcare resources [7-11]. In order to improve the fetal diagnosis of CoA by reducing the proportion of false positives, a number of fetal echocardiographic predictors of postpartum CoA have been proposed. These include diameters, Z-scores and ratios between right and left heart structures, as well as flow anomalies across the atrial septum and aortic arch [9,12-16].

Of these, mitral and aortic valve or aortic isthmus Z-scores, the ratio of right-to-left ventricular, pulmonary artery-to-ascending aorta, and isthmus-to-duct diameters, as well as the presence of a posterior shelf or aortic arch hypoplasia, were most predictive of postpartum CoA, as shown in a systematic review of more than 900 fetuses with suspected CoA [17]. Of note, flow anomalies across the atrial septum and/or aortic arch and the concomitant presence of minor CHDs such as L-SVC, BAV or VSD were not significantly associated with postpartum CoA [17].

The use of additional fetal echocardiographic variables including aortic arch angles [16,18], or more advanced imaging techniques such as 3D/4D fetal echocardiography, speckle tracking or fetal cardiac magnetic resonance imaging (fetal CMR) [19-21] have been proposed to improve the prenatal diagnosis of CoA.

The vast majority of fetuses with suspected CoA and borderline left heart structures will have a biventricular outcome due to the potential for growth with cardiac filling. This is particularly true in cases without associated left-sided valvar disease of significance [22,23].

Is the prenatal formation of CoA flow dependent?

The intrauterine conditions leading to the postnatal development of CoA are not fully understood. The hemodynamic theory suggests a progressive underdevelopment of the left heart structures, including the aortic arch, due to reduced intrauterine flow through the left heart [24]. However, the origin of the formation of a posterior shelf with an increased distance between the left carotid and subclavian artery has not been fully elucidated (*Figure 3*). A markedly reduced to reversed flow in the aortic isthmus may lead to its anatomic formation [25]. However, another theory suggests the involution and subsequent upward shift of a small segment of the posterior aortic wall together with the left subclavian artery as the source of the aforementioned anatomic changes [26].

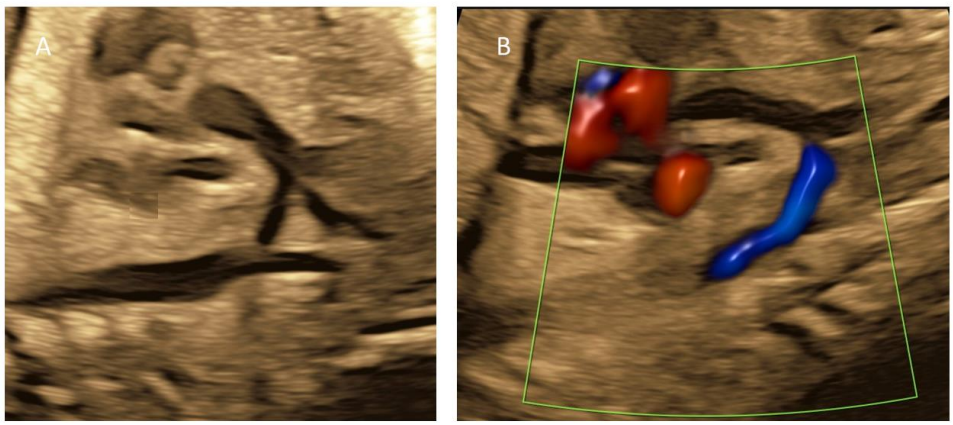

Figure 3: Fetus at 27 weeks of gestation with suspected CoA. A) Sagittal view showing hypoplasia of the aortic arch with a long distance between the left common carotid and the left subclavian artery. B) Continuous diastolic forward flow in the aortic arch as a non-specific sign of coarctation of the aorta.

Improved fetal diagnosis of suspected left heart obstructions including CoA using fetal CMR flow assessment?

A recent fetal CMR study indicated an association between reduced flow in the ascending aorta and changes in the aortic arch configuration with postpartum CoA formation [21]. However, imaging of the ascending aorta with reliable flow measurements is challenging, whereas quantification of blood flow in the descending aorta (DAo) is valid and reproducible [27].

Neonatal management when CoA is suspected prenatally

Fetuses with suspected CoA should be scheduled for delivery in a centre with access to pediatric cardiology expertise with thorough neonatal monitoring including serial clinical and echocardiographic examinations. Prostaglandins should be administered if critical CoA is confirmed with ductal closure or if there is marked hypoplasia of the aortic arch or aortic isthmus immediately after birth. When the neonatal diagnosis of CoA cannot be made with certainty because of a persistent arterial duct, the carotid-subclavian artery index (CSAI), defined as the ratio of the distal aortic arch diameter to the distance between the left common carotid and left subclavian artery, may help to identify neonates at risk of CoA [28]. In some cases, more advanced imaging techniques such as computed tomography (CT) or magnetic resonance imaging (MRI) may be required to determine the anatomy of the aortic arch and any associated intra- and extracardiac malformations.

Neonatal repair of CoA

The surgical approach of choice for neonates with isolated CoA is a lateral thoracotomy with either an end-to-end or extended end-to-end anastomosis [29]. Of these, the extended end-to-end anastomosis, a modification of the end-to-end anastomosis, connects the proximal to the distal segment of the aorta in an overlapping fashion to enlarge the distal aortic arch [30]. More complex cases with concomitant VSD in need of neonatal repair or cases with marked aortic arch hypoplasia are predominantly corrected via median sternotomy on cardiopulmonary bypass. For the latter, an end-to-side anastomosis or aortic arch repair with patch material, may be chosen (*Figure 4*) [31-33]. In our centre, surgical modifications with transitions between the different surgical methods are used at times.

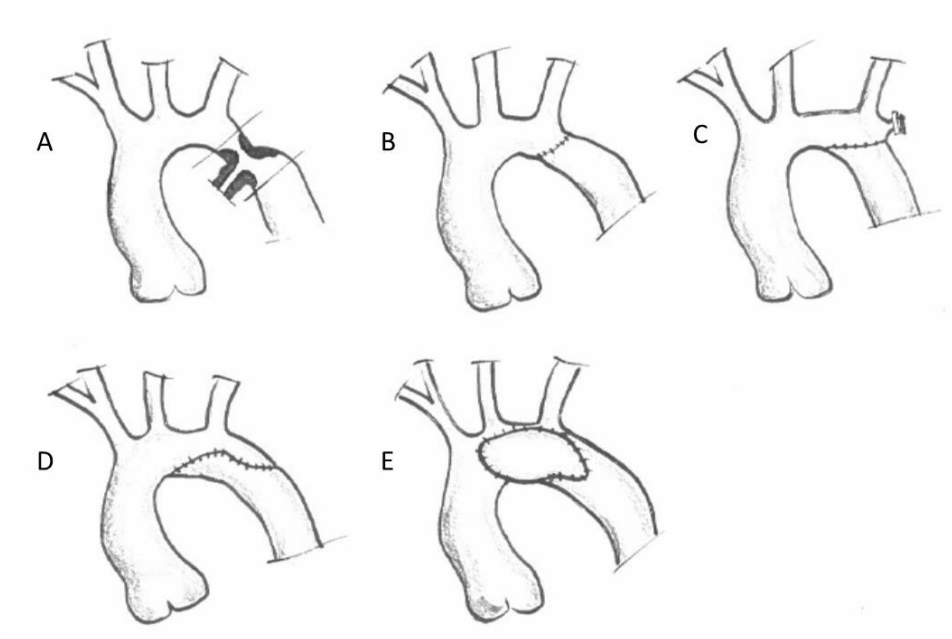

Figure 4: Examples of CoA repair techniques: A) Simple CoA with focal narrowing prior to surgery, B) End-to-end anastomosis, C) End-to-side anastomosis, D) Extended end-to-end anastomosis, E) Patch aortoplasty. *Illustration by Dr. Phan Kiet Tran, lead surgeon, Pediatric Heart Centre, Lund, Sweden.*

Complications after surgery

In the current era, outcomes after CoA repair are usually good with low perioperative mortality rates [34]. However, there are a number of short- and long term complications that need to be considered. Short term complications include residual gradients in the aortic arch after CoA repair, which may contribute to progressive LV hypertrophy and pulmonary hypertension, if located proximally [32]. Another well-known sequela is arterial hypertension, which occurs in up to 15-30% of children following CoA repair [34,35]. Anomalous aortic wall properties with increased arterial stiffness, dysregulation of the renin-angiotensin-aldosterone system or aortic baroreceptors, residual hypoplasia with or without focal aortic arch stenosis, and certain types of aortic arch geometry after CoA repair may contribute to its development [36-40]. Other rare complications that may occur later in life include aortic aneurysm formation and myocardial dysfunction [29].

Recurrent coarctation (re-CoA)

Re-CoA is a common complication after CoA repair, occurring in approximately 10-20% of patients [41,42]. Most cases present within months after neonatal CoA repair. A variety of risk factors have been proposed, including neonatal repair itself or young age and low preoperative weight at neonatal repair [34,43]. Repair technique may also play a role, with extended end-to-end anastomosis via lateral thoracotomy appearing to be superior to end-to-end anastomosis [31,44-46]. More extensive repair techniques including end-to-side anastomosis or arch repair techniques using autologous patch material, may also reduce the risk of re-CoA [32,47,48]. Interestingly, another study found an increased risk of re-CoA, when patch material was used [49]. Residual postoperative hypoplasia of parts or the entire aortic arch may contribute to the formation of re-CoA [32,41,49-51]. Increased postoperative isthmic Doppler gradients and arm-leg blood pressure gradients prior to discharge, have been reported in infants who developed re-CoA [52,53].

In addition, the shape of the aortic arch after CoA repair may also play a role. A previous study has found an association between a pointed (gothic) or rectangular (crenel) arch, and an increased risk of re-CoA [54]. However, the classification into three aortic arch shapes is an oversimplification and more complex models may be needed to more accurately assess aortic arch geometry.

Hypoplastic left heart syndrome (HLHS)

Background

HLHS is a duct-dependent major CHD in which the left ventricle is unable to supply the systemic circulation and accounts for approximately 3% of all CHDs [55]. Despite improvements in fetal diagnosis, surgical technique and perioperative care, HLHS remains a critical cardiac condition associated with short- and long term morbidity and mortality [56].

Surgical approach

Staged univentricular palliation has transformed HLHS from a fatal cardiac condition to a treatable one. Palliative surgery in patients with HLHS was first described in 1980 [57] and has been performed in Sweden since 1993. Over time, various surgical modifications along with advances in perioperative care have led to a dramatic improvement in neonatal survival [58].

Univentricular palliation for HLHS involves a series of three surgical stages aimed at separating the pulmonary from the systemic circulation, with the right ventricle pumping saturated blood into the systemic circulation while desaturated blood from the upper and lower body passively reaches the lungs, bypassing the heart. Various surgical modifications have been proposed for the three stages. Briefly, the Norwood stage I procedure (stage I), the bidirectional Glenn (stage II) and the total cavopulmonary connection (TCPC; stage III) with extracardiac conduit, are usually performed (*Figure 5*). The Norwood stage I procedure involves the 1) creation of an unobstructed connection from the right ventricle (RV) to the systemic circulation by reconstructing the aortic arch to the right ventricular outflow tract; 2) creation of an unobstructed communication between the left and the right atria, and 3) creation of a systemic-to-pulmonary shunt to facilitate pulmonary blood flow. In the second stage, a Glenn anastomosis is performed to redirect desaturated blood from the upper body through the superior vena cava directly into the pulmonary arteries. Finally, the third stage completes the anatomic separation of the pulmonary and systemic circulations by redirecting venous blood flow from the lower body to the lungs (*Figure 5*).

As part of the Norwood procedure, either a modified Blalock-Taussig (BTs) or Sano shunt can be utilized. The Sano shunt modification was introduced in 2002 with the aim of improving early postoperative outcomes by preventing diastolic runoff and subsequent coronary steel [59]. However, ventriculotomy is required to connect the conduit from the RV to the pulmonary artery, which theoretically may affect short- and long term right ventricular performance [60].

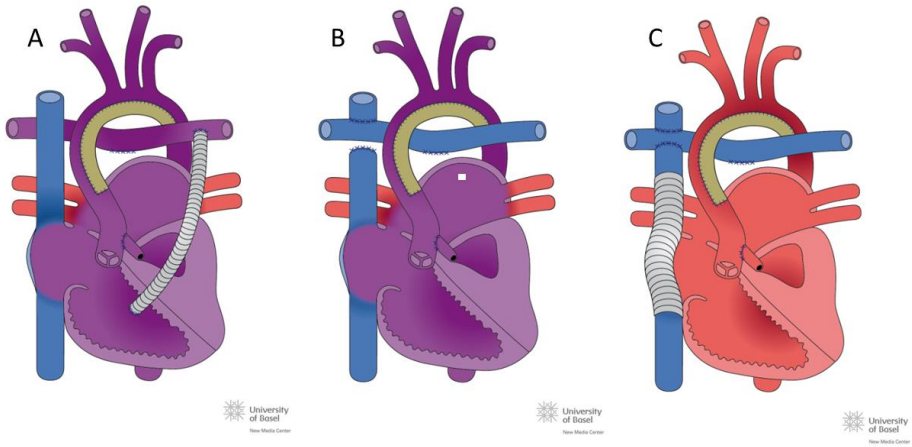

Figure 5: Staged univentricular palliation. A) Stage I Norwood procedure with Sano shunt, B) Glenn anastomosis, C) Total cavopulmonary connection (TCPC). *Illustration taken from Congenital Heart Disease (congenital-heart-disease.ch).*

Fetal diagnosis of HLHS

Fetal diagnosis of HLHS allows for optimal counselling, planning of delivery and perinatal care, contributing to decreased neonatal morbidity and mortality [61]. As a result of improved fetal screening, the detection rate of univentricular heart defects in Sweden has increased to approximately 80-90% over the last decades, although with regional variations (SWEDCON/Fetal Report 2022). Termination of pregnancy in univentricular hearts has reached a current rate of 74% (SWEDCON/Fetal Report 2022; cumulative termination rates 2014 to 2022).

HLHS is relatively easy to detect with fetal echocardiography because of the underdeveloped left ventricle seen in the four-chamber view, the most basic screening view (*Figure 6A*). However, visualization of the usually diminutive ascending aorta and aortic arch in the outflow tract views is more challenging. The use of colour Doppler may be helpful here, as it can show retrograde flow in the aortic arch (*Figure 6B*). Attention must also be paid to right ventricular function, the presence of significant tricuspid regurgitation and the adequacy of the interatrial communication, all of which may affect perinatal outcome.

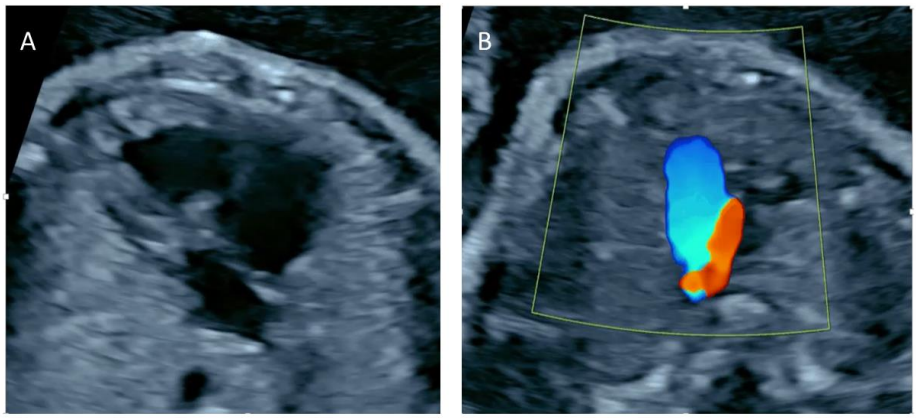

Figure 6: Fetus with HLHS with a slit-like left ventricle, aortic and mitral atresia (AA-MA) and aortic arch hypoplasia. A) Four-chamber view showing two atria and the right venticle. The slit-like left ventricle is not visible. B) Three-vessel trachea view: colour Doppler demonstrates retrograde (red) flow in the hypoplastic aortic arch and antegrade (blue) flow in the ductal arch.

Intrauterine fetal demise (IUFD), which occurs sporadically in fetuses with HLHS, may appear in the presence of concomitant cardiac or extracardiac malformations or genetic anomalies [62]. Fetal risk factors for poor neonatal outcome involve the simultaneous occurrence of genetic or extracardiac comorbidity, as well as the presence of significant tricuspid regurgitation [63] or a highly restrictive (RAS) or intact atrial septum (IAS) [64]. RAS/IAS impedes blood egress from the left atrium, resulting in increased left atrial pressures, pulmonary venous congestion and ultimately pulmonary vasculopathy and lymphangiectasia, a condition highly associated with neonatal morbidity and mortality (*Figures 7 and 8*) [65].

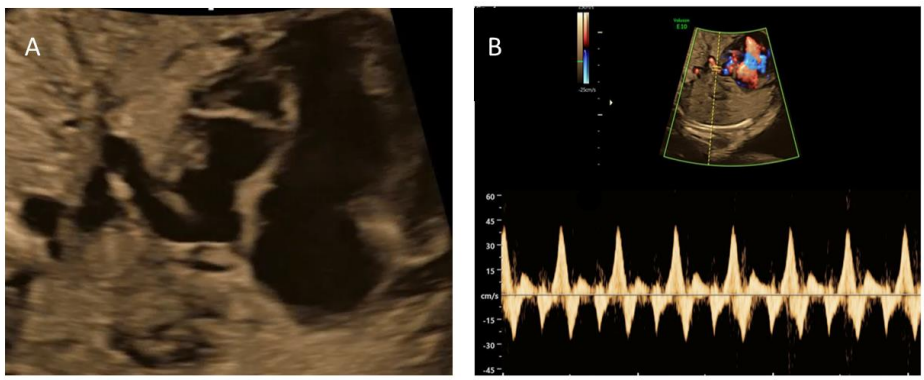

Figure 7: Fetus with HLHS and an intact atrial septum. A) Four-chamber view demonstrating HLHS with intact atrial septum and dilated pulmonary veins. B) Pulmonary venous flow pattern with significant flow reversal with atrial contraction indicating profound interatrial restictivity.

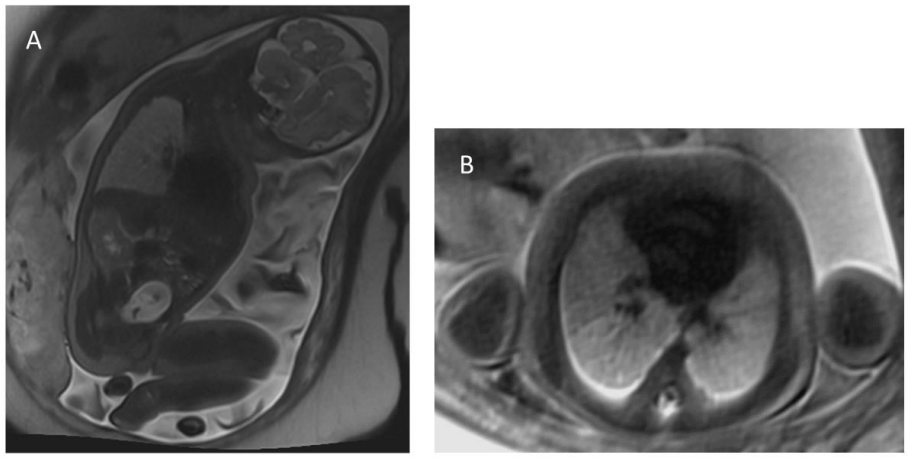

Figure 8: Fetal MR imaging of a fetus with HLHS and intact atrial septum. Figure 8 A) and B) show signs of mild pulmonary lymphangiectasia (nutmeg lung pattern), while B) also shows bilateral pleural effusion.

Once the diagnosis has been made, comprehensive counselling needs to take into account the likely intrauterine, neonatal, short- and long term outcomes. If the family wishes to continue the pregnancy, regular follow-up examinations are crucial in order to monitor the condition of the fetus and ultimately being able to plan for optimal delivery and perinatal care.

Fetuses with suspected HLHS are usually planned for vaginal delivery in a tertiary centre with unhindered access to pediatric heart surgery and optimal perioperative care. In our centre, caesarean section is reserved for high risk pregnancies including fetuses with suspected RAS/IAS (with cath-lab on hold) or, less commonly, other conditions that may lead to clinical deterioration during delivery. In cases with expected adverse outcome, where the univentricular palliative pathway is rendered unsuitable, vaginal delivery and neonatal comfort care may be an alternative option.

Short-and long term outcome

Mortality

With advances in surgical technique and perioperative care, survival has improved significantly over the past few decades. In the recent era, 30-day mortality rates as low as 12% [66] and interstage I mortality rates of 11% [67] have been observed in experienced centres. Mortality associated with stages II and III is generally low, and 10-year survival after stage III is estimated to be around 90% when operated in the recent era [68]. Current data from our centre indicate a favorable short- and long term outcome with 2.2% 30-day mortality, 4.4% 90-day mortality, 5.5% interstage I mortality, with an overall HTx-free survival of approximately 80% over the last two decades (unpublished data).

Morbidity

Despite the success story of decreasing, particularly perioperative neonatal mortality, HLHS is still burdened with significant short- and long term morbidity. More than 50% of Fontan patients will experience major adverse events before reaching adulthood, including thromboembolic events, supraventricular tachycardia, heart failure, or the need for reoperation, intervention, or pacemaker implantation [68]. Secondary diseases resulting from the increased systemic venous pressure and chronically decreased cardiac output are known problems of the Fontan circulation [69]. Fontan-associated liver, kidney and lung disease, including liver congestion, protein-losing enteropathy (PLE), pulmonary vasculopathy and coagulopathies may develop over time [69]. Neuropsychiatric sequelae such as attention deficit disorder, executive dysfunction, memory problems and mental illness in later life [70], as well as reduced exercise capacity, are common findings in patients with Fontan circulation. In addition, the development of systemic ventricular dysfunction with or without atrioventricular regurgitation is a serious problem that needs to be addressed [69]. Ultimately, heart transplantation may be the only treatment option for intractable heart failure or Fontan circulation failure.

Anatomic and morphological LV subtypes

The anatomic HLHS classification relates to mitral and aortic valve patency and encompass the following three subtypes: aortic and mitral valve atresia (AA-MA), aortic valve atresia and mitral valve stenosis (AA-MS), and aortic and mitral valve stenosis (AS-MS). Other subtypes involving a non-restrictive VSD are not included in this classification [71]. The impact of the above anatomic subtypes on clinical outcome has been extensively studied, however, with conflicting results. Earlier studies linked AA-MA to adverse outcomes [72-74], whereas more recent studies have associated AA-MS with increased short- and long term mortality [75-77].

In the literature, three morphological left ventricular phenotypes have been identified in patients with HLHS: A) a slit-like LV, difficult to identify on transthoracic echocardiography, B) a globular, thickened LV with endocardial fibroelastosis (EFE), and C) a miniaturized, non-apex forming LV with normal myocardial thickness in the absence of EFE (*Figure 9*) [78,79].

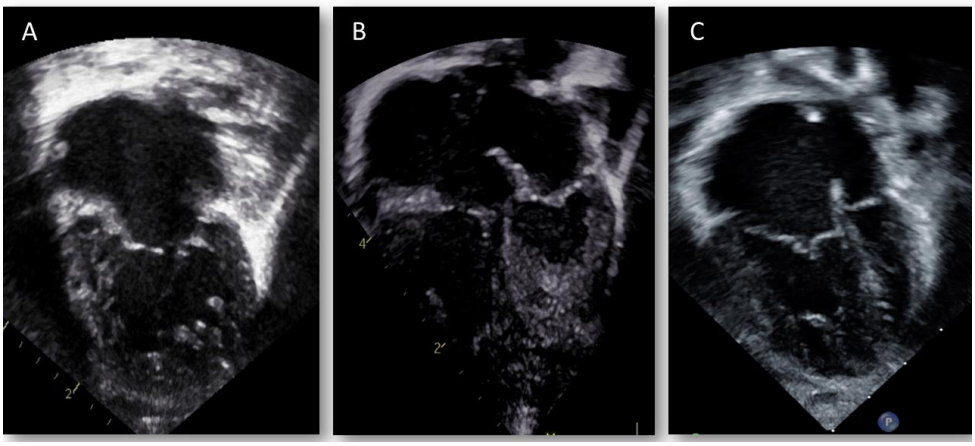

Figure 9: Left ventricular phenotypes. A) Slit-like left ventricle. B) Globular left ventricle. C) Miniaturized left ventricle. *Figure from Fricke et al., JAHA 2022 [80] licensed by* *https://creativecommons.org/licenses/by-nc/4.0/*

A slit-like LV is found only in patients with AA-MA, whereas a miniaturized LV is found only in patients with AS-MS with moderately underdeveloped left ventricular in- and outflow. The globular LV phenotype is the most common and predominantly found in AA-MS, but also in the AS-MS subtype with critical outflow tract obstruction [78,79].

The impact of LV morphology on RV function and outcome has not yet been conclusively clarified. It has been suggested, that a larger residual LV and/or a hypertrophied ventricular septum may adversely affect systemic right ventricular function and outcome [81-84].

Other risk factors for adverse outcome

In addition to genetic, functional, morphological, early surgical or associated cardiac and extracardiac malformations, prematurity and low preoperative weight (≤2.5 kg) at Norwood stage I, as well as the era in which surgery was performed, have been described as risk factors for adverse, predominantly short term outcome [85,86].

Aims

The overall aim of this thesis was to improve the prenatal diagnosis and outcome in patients with left heart anomalies.

The aims of the individual studies were as follows:

Paper I

To identify fetal echocardiographic predictors of postpartum CoA in fetuses with suspected CoA.

Paper II

To assess the association of left ventricular morphology and neonatal surgical factors with morbidity and mortality in patients with HLHS following Norwood stage I palliation.

Paper III

To assess whether the addition of fetal CMR of the descending aorta and umbilical vein to fetal echocardiography improves the fetal detection of left heart obstructions requiring neonatal intervention.

Paper IV

To characterize aortic arch geometry and blood flow in neonates following CoA repair by magnetic resonance imaging and to compare these two between neonates with and without the occurrence of re-CoA within the first year of life.

Methods

Paper I

This single-institution, retrospective fetal echocardiography study included infants born between 2010 and 2018 with prenatally suspected CoA. Suspicion of CoA was predominantly based on disproportion at the level of the ventricles and/or great arteries. Fetuses with associated CHDs other than L-SVC, mild mitral (MS) or aortic valve stenosis (AS), hypoplastic aortic arch, or suboptimal visualization of the aortic arch were excluded. Medical and operative reports were searched for information on suspected prenatal diagnosis, intrauterine course and perioperative outcome.

Fetal echocardiographic measurements

Fetal echocardiographic measurements of left and right heart structures, including isthmic and ductal dimensions in the sagittal and three-vessel trachea (3VT) views, were conducted. The CSAI, which is the ratio of the distal aortic arch diameter before the take-off of left subclavian artery to the distance between the left common carotid artery and the left subclavian artery, was also calculated (*Figure 10*). Fetal cardiac Z-scores [87-90] were applied and the following ratios between the left and right heart structures were computed: left-to-right ventricular (LV/RV) width and length, mitral-to-tricuspid valve diameter (MV/TV), aortic-to-pulmonary valve diameter (AoV/PV), ascending-to-descending aortic diameter (AAo/DAo) and isthmus-to-duct diameter (I/D) in the the 3VT and sagittal views (*Figure 10*).

All quantitative measurements and qualitative analyses were conducted by a single observer (KF).

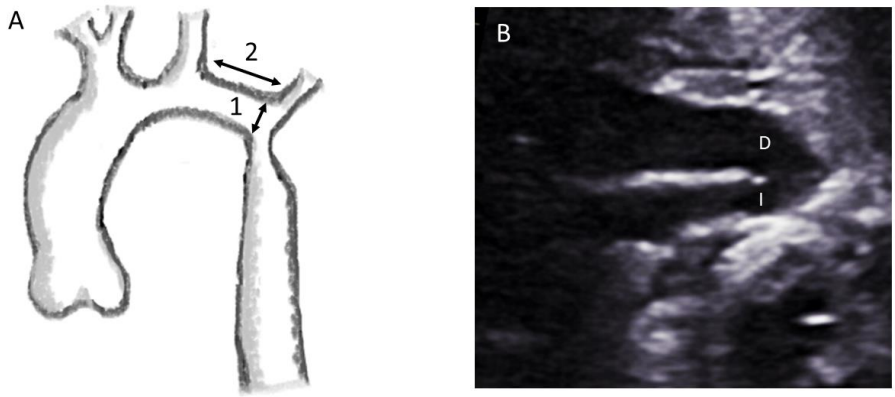

Figure10: A) Carotid-subclavian artery index (CSAI): ratio of 1) The aortic arch diameter at the take-off of the left subclavian artery to 2) The distance between the left common carotid artery and the left subclavian artery. *Illustration by Dr. Katrin Fricke.* B) Isthmus-to-duct ratio (I/D) in the three-vessel trachea view.

Statistics

Data were presented as mean and standard deviation (SD) or median and interquartile range (IQR). The χ^2- or Fisher´s exact test, Mann–Whitney U test, paired sample T-test, logistic regression analyses and odds ratios (95% confidence interval) were applied depending on the type of variable and research question. Cut-off values with corresponding sensitivity and specificity were calculated for the fetal echocardiographic variables most predictive of postpartum (true) CoA. In addition, receiver operating characteristic (ROC) curves were provided. *P* values of <0.05 were regarded as statistically significant. For statistical analyses, the Statistical Package for Social Sciences, version 25 (IBM SPSS, Chicago, IL) was used.

Paper II

This retrospective, nationwide study included patients with HLHS after Norwood stage I palliation between January 1999 and December 2018. All anatomic HLHS subtypes other than AA-MA, AA-MS, and AS-MS, and patients with a non-restrictive ventricular septal defect were excluded. Eligible patients were identified from SWEDCON (Swedish Registry of Congenital Heart Disease) or the local institutional surgical databases of the two centres, Lund and Gothenburg that perform pediatric heart surgery in Sweden. Surgical and perinatal clinical reports were searched for data on demographics, perinatal as well as short- and long term postoperative outcomes.

Echocardiographic assessment

Available fetal, pre-and postoperative echocardiograms were reviewed for anatomic and functional details by a single observer (KF). The following three anatomic HLHS-subtypes were identified: A) AA-MA (no flow across the aortic and mitral valve), B) AA-MS (flow across the mitral valve only), and C) AS-MS (flow across both the aortic and mitral valve). Left ventricular phenotypes were defined as A) slit-like (thin-walled LV with a slit-like cavity), B) globular (with a thickened, hypoplastic, non-apex forming LV with EFE) and C) miniaturized (with a non-apex forming, hypoplastic LV without EFE or myocardial hypertrophy) (*Figure 9*).

The presence of 1) a highly restrictive atrial septum (RAS), defined as a mean gradient across the atrial septum of ≥8 mm Hg [91] and/or a small-sized atrial septal defect with an explicit preoperative clinical presentation, or 2) an intact atrial septum (IAS: no flow across the atrial septum) was assessed. The degree of RV dysfunction (mild to moderate) and tricuspid valve regurgitation (moderate to severe) was assessed at the last echocardiogram or echo report before Norwood stage I palliation.

Other perinatal risk factors including postnatal diagnosis, female sex, prematurity (<37 weeks of gestation), low preoperative weight (≤2.5 kg), RV dysfunction, RAS or IAS before Norwood stage I, as well as cardiac and extracardiac comorbidity and early surgical factors such as shunt type at Norwood stage I, were assessed.

Outcome variables

Outcome variables included:

A) Mortality

1. Overall operative mortality within 30 days of surgery and/or before hospital discharge after Norwood stage I
2. Interstage I [IS-I]
3. Interstage II [IS-II]
4. Post-TCPC and

B) "Major adverse events" (MAE), a combined morbidity/mortality variable. MAE included need for left ventricular assist device (LVAD) or extracorporeal membrane oxygenation (ECMO), protein-losing enteropathy (PLE), takedown of Glenn or TCPC, heart transplantation (HTx), and overall mortality.

Statistics

Data were presented as median and range. Statistical analyses included the Mann-Whitney U or Kruskal-Wallis test (for continuous variables) and the $\chi 2$- or Fisher´s exact test (for categorical variables). The Wilcoxon log-rank test and Cox regression (95% CI) were used to assess differences in survival or freedom from MAE between the groups. A stepwise multivariate Cox regression model was applied, including variables with a *P* value of ≤ 0.2. A Cox regression model was also used to test for an interaction between LV morphology and Norwood stage I shunt type. Kaplan-Meier curves were provided. A *P* value of <0.05 was considered statistically significant. The Statistical Package for Social Sciences version 25 (IBM SPSS, Chicago, IL) and StatView 5.01 for Windows (SAS Institute, Cary, NC) were used for statistical analyses.

Paper III

For this prospective, single-institution study, pregnant women with fetuses suspected of having left heart obstructions (HLHS, critical aortic stenosis (cAS), CoA) and healthy controls were recruited between October 2017 and August 2022. With respect to the study objectives, fetuses were further categorized into A) those with left heart obstructions requiring postpartum cardiac intervention versus all others; B) those with retrograde systolic isthmic flow (as a potential marker of severe left heart obstruction) versus all others; and C) fetuses with suspected CoA with (true CoA) and without (false positive CoA) requiring postpartum intervention.

All fetuses underwent a detailed fetal echocardiogram and fetal CMR, usually on the same day.

Fetal echocardiographic assessment

Fetal echocardiographic measurements were carried out by a single observer (KF). Ratios, highly predictive of true CoA in our retrospective fetal echocardiography study, were calculated [92]. Atrial septum appearance (normal, redundant, restrictive or intact), isthmic flow velocity, isthmic flow direction (antegrade, bidirectional, retrograde), presence of a posterior shelf and maximum diaphragmal DAo diameter, were also assessed. Associated cardiac anomalies were noted. The following definitions were used: 1) RAS in fetuses with suspected CoA: hardly any right-to-left shunt across the atrial septum as assessed by colour Doppler; 2) RAS in fetuses with cAS or HLHS: antegrade-to-retrograde pulmonary venous velocity time integral (VTI) ratio of ≤ 3 [93]; 4) retrograde systolic isthmic flow: flow reversal in systole; 5) bidirectional isthmic flow: flow reversal in end-systole or diastole.

Fetal CMR assessment

Phase-contrast fetal CMR-derived quantification of blood flow in the DAo and umbilical vein (UV) was conducted at 1.5 T Aera (Siemens, Erlangen Germany) and gated by Doppler ultrasound (smart-sync; Northh Medical, Hamburg, Germany) in non-breathhold [94]. Flow measurements were normalized for fetal weight derived from 3D CMR [95] and DAo upslope and downslope for net flow. Segment version 3.3 (Medviso AB, Lund, Sweden) was used for image analyses [96]. Two observers carried out all measurements (KF, DR).

All observers were blinded to the postoperative clinical outcome.

Fetal growth restriction (FGR) was defined as an estimated fetal weight below the 10th percentile for gestational age.

Fetuses with suspected left heart obstructions were scheduled for delivery at our tertiary centre. Those with HLHS or cAS and suspected RAS or IAS were planned for delivery by caesarean with cath-lab on hold. Neonates with prenatally suspected CoA were carefully monitored until CoA was confirmed or ruled out.

Prostaglandins were administered in cases of confirmed neonatal CoA and in those with severe left heart obstructions and duct-dependent systemic circulation.

Statistics

Data were presented as median and interquartile range (IQR). The Mann–Whitney U or the Kruskal–Wallis test was applied to compare continuous variables and the χ^2 test or Fisher's exact test was used to compare categorical variables. Intraclass correlation coefficients (ICC) with 95% confidence intervals were considered excellent if an ICC of >0.90 was obtained with corresponding confidence interval [97]. A *P* value of <0.05 was considered statistically significant. Statistical analyses were performed using the Statistical Package for Social Sciences version 28 (IBM SPSS, Chicago, IL).

Paper IV

In this prospective, single-institution study, we included neonates who had CoA repair between November 2018 and February 2023. All underwent a detailed postoperative transthoracic echocardiogram and cardiac MRI before discharge.

Exclusion criteria were suboptimal MR imaging and associated CHDs other than aortic arch hypoplasia, borderline LV, VSD and BAV.

Multiple preoperative transthoracic echocardiograms and, if needed, CT scans were performed to establish the diagnosis and identify associated minor cardiac malformations.

Neonates with associated marked aortic arch hypoplasia and/or VSDs requiring neonatal repair underwent median sternotomy. Lateral thoracotomy was performed in all other cases.

MRI assessment

MRI examinations were performed on a 1.5T Aera scanner (Siemens Healthcare, Erlangen, Germany), using the "feed-and-sleep" method, with support of chloral hydrate, if needed (25 mg/kg, APL, Sweden; rectal application) [98]. Four-dimensional (4D) flow volumes and T1-weighted black blood 3D sequences were applied, and image analysis was performed using Segment version 3.3 (Medviso AB, Lund, Sweden) [96]. All observers were blinded to the postoperative clinical outcome.

Assessment of aortic arch geometry

A 3D model of the aortic arch was generated from black blood images by using Segment 3D Print (Medviso AB, Lund, Sweden).

Aortic arch shape

The shape of the aortic arch was classified as A) roman (round), B) crenel (rectangular with a long transverse aortic arch segment), or C) gothic (pointed with a short distance between the ascending and descending aorta) *(Figure 11)* [40].

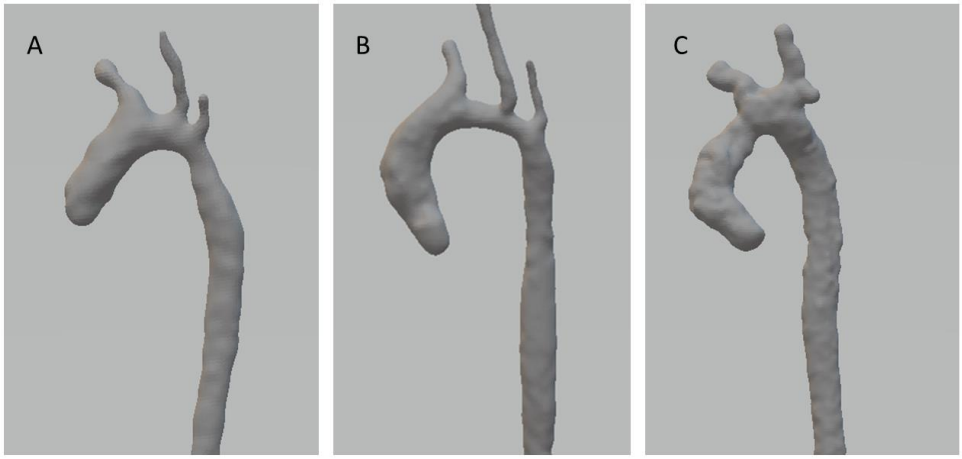

Figure 11: Subtypes of postoperative aortic arch shapes. A) Roman, B) Crenel, C) Gothic.

3D angles

Centrelines of the aortic arch and head-neck vessels were calculated. Vectors to the branching points were calculated to compute angles between the ascending and descending aorta and the aortic arch to the branching points as well as the anteroposterior angulation of the aortic arch. The distance between the first and last branching points was calculated as well. All 3D angle calculations were performed by a single observer (LC). The calculated 3D angles are shown in *Figure 12*.

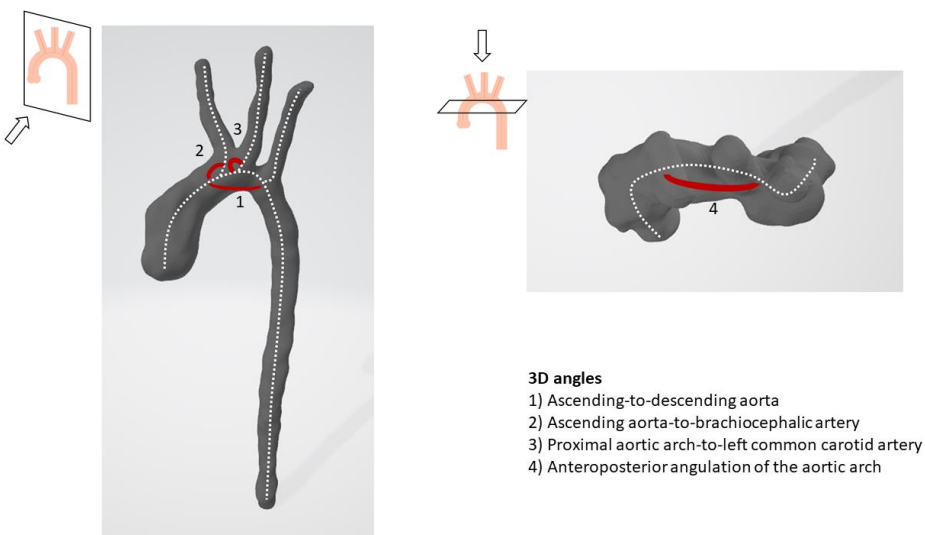

Figure 12: 3D angles of the aortic arch

Calibre change from the distal ascending aorta to the aortic isthmus

The areas of the distal ascending aorta, the proximal and the distal aortic arch and the isthmus were measured proximal to the origins of the head-neck vessels and at the isthmus, respectively. The ascending aortic area was correlated with the other three area measurements. All measurements were performed by a single observer (KF).

Assessment of flow pattern in the distal aortic arch

Flow measurements were conducted in the distal aortic arch between the origin of the left common carotid artery (or innominate artery in the case of a bovine arch) and 2 cm distal to the origin of the left subclavian artery (*Figure 13A*). Helicity and vorticity were calculated quantitatively using an in-house plug-in to the Segment software, implementing the vector pattern matching method of Heiberg *et al. (Figure 13B)* [99]. All flow measurements were performed by a single observer (KF).

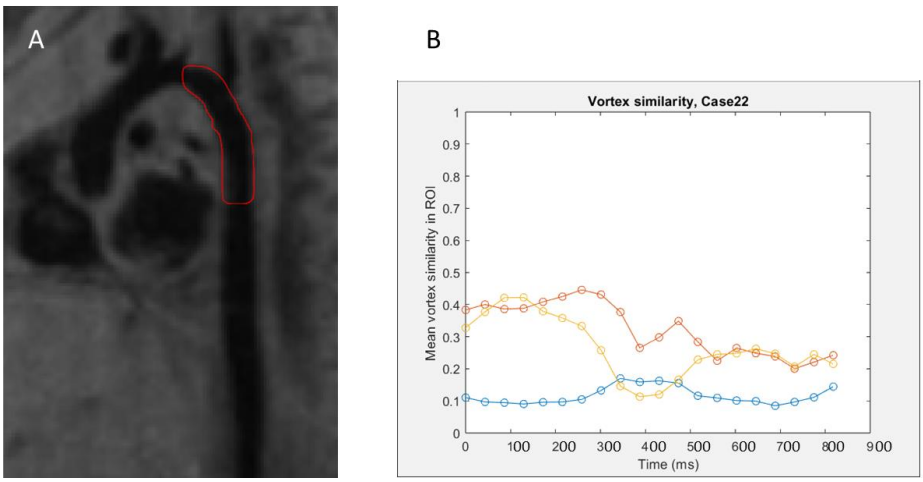

Figure 13: Flow measurements in the distal aortic arch. A) Black blood image showing the measurement area (red). B) Output related to mean similarity of the flow pattern over one cardiac cycle, with the red line representing right-handed helicity, the yellow line representing left-handed helicity and the blue line representing vorticity.

Outcome

Re-CoA was defined as a narrowing of the aortic arch requiring re-intervention within the first 12 months after CoA repair.

Statistics

Data were presented as median and interquartile range (IQR). Group-wise comparison was done by applying the Mann-Whitney-U test for continuous variables and the χ^2 test or Fisher´s exact test for categorical variables. For linear relation, Pearson´s correlation was used. *P* values of <0.05 were considered statistically significant and those of ≥ 0.05 and <0.1 were considered to indicate a trend. The Statistical Package for Social Sciences, version 29 (IBM SPSS, Chicago, IL) was used for data analysis.

Results

Paper I

Title: Fetal Echocardiographic Dimension Indices: Important Predictors of Postnatal Coarctation

The aim of this study was to improve the prenatal diagnosis of CoA using fetal echocardiography.

Study population and patient characteristics

After exclusion of 12 fetuses due to suboptimal fetal echo quality, 65 fetuses could be analysed, of whom 22 (34%) developed CoA postnatally. Four neonates had to undergo Norwood stage I palliation due to significant associated left heart obstructions. All patients with true CoA underwent surgical repair in the neonatal period, with either end-to-end repair (n=4), end-to-side repair (n=11) or aortic arch reconstruction (n=3).

Fetuses were usually referred for fetal echocardiography, because a disproportion of the ventricles or great arteries was detected at the fetal screening. The fetal echocardiogram used for analysis was performed at a mean gestational age of 34.1 (26.3-39.3) weeks. Associated cardiac anomalies included borderline left heart structures (n=44), aortic arch hypoplasia (n=22) or the presence of L-SVC (n=7), mild MS (n=1) or AS (n=2) and VSD (n=10). Associated extracardiac or genetic anomalies were found in three and one fetuses, respectively.

Qualitative and quantitative fetal echocardiographic assessment

Fetuses with postnatally confirmed CoA had significantly smaller left heart structures and lower ratios between the left and right heart structures than those not requiring neonatal aortic arch surgery (false positives). Logistic regression analyses and ROC curves were provided for fetal echocardiographic variables significantly associated with true CoA (*Figure 14*). Of these, both a CSAI of less than 0.78 (sensitivity 92%, specificity 97%) and the product of the isthmus-to-duct (I/D) ratio

in the 3VT view and the mitral-to-tricuspid valve (MV/TV) ratio in the four-chamber view (I/D3VTxMV/TV) of less than 0.37 (sensitivity 100%, specificity 95%) were most predictive of postpartum CoA.

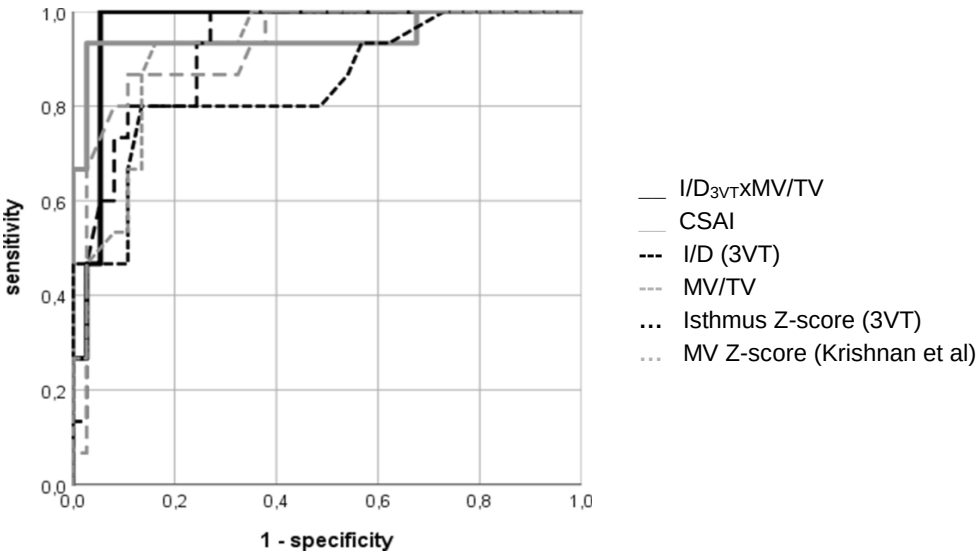

Figure 14: ROC curve for fetal echocardiographic variables associated with postpartum CoA. I/D_{3VT}xMV/TV: product of isthmus-to-duct ratio in the three-vessel trachea (3VT) view and mitral-to-tricuspid valve ratio in the four-chamber view; CSAI: carotid-subclavian artery index; I/D (3VT): isthmus-to-duct ratio in the 3VT view; MV/TV: mitral-to-tricuspid valve ratio. *Illustration reproduced from Fricke et al., Pediatr Cardiol. 2021*[92]*, licensed by https://creativecommons.org/licenses/by/4.0/*

Borderline left heart structures, the presence of an aortic arch hypoplasia, posterior shelf or VSD, and flow anomalies across the atrial septum or in the aortic arch were also associated with true CoA ($p \leq 0.002$).

Unexpectedly, there were significant differences in the Z-score data sets of up to a mean of 2.9 for the same measurements of left and right heart structures.

In the prospective validation of 16 fetuses with suspected CoA, born in 2019, a CSAI with a cut-off of <0.78 and I/D_{3VT}xMV/TV of < 0.37 detected those developing CoA in the neonatal period with high sensitivity and specificity (100% & 91%; 100 & 100%, respectively).

Paper II

Impact of Left Ventricular Morphology on Adverse Outcomes Following Stage 1 Palliation for Hypoplastic Left Heart Syndrome: 20 Years of National Data From Sweden

This study aimed to investigate the impact of left ventricular morphology and choice of Norwood stage I shunt type on short- and long term morbidity and mortality in patients with HLHS.

Study population and patient characteristics

One hundred and sixty-seven patients with HLHS and after Norwood stage I palliation met the inclusion criteria. Cardiac comorbidity was encountered in 9 patients, 4 of whom had partial or total anomalous pulmonary venous drainage. None of them died during follow-up, but 2 had MAE. Extracardiac anomalies were found in 10 patients (*Table 1*).

Forty-six patients (28%) underwent a Norwood stage I palliation with a BTs. Preferential but not exclusive use of the Sano shunt was observed after its introduction in 2002. Overall mortality during follow-up was 31%, consisting of 10% operative mortality, 19% interstage I mortality, 13% interstage II mortality, and 5% post-TCPC mortality. MAE occurred in 41%, predominantly consisting of the need for ECMO/LVAD and mortality (*Table 1*).

Left ventricular morphology

The most common anatomic subtype was AA-MA (41%), followed by AA-MS (35%) and AS-MS (25%) (*Table 1*). Among the LV phenotypes, a globular LV was the most common (58%), observed in all patients with AA-MS, in more than half of those with AS-MS (61%) and 19% of those with the anatomic subtype AA-MA. In contrast, a slit-like LV was present in 33% of patients and only in the anatomic subtype AA-MA, whereas a miniaturized LV was present in 10% of patients and only in AS-MS (*Table 2*).

Perinatal variables were evenly distributed between the anatomic and LV phenotype subgroups, except for female sex, which was most common in patients with a slit-like LV (*Tables 1 and 2*). Norwood stage I palliation with a BTs was more frequently performed in patients with AS-MS or a miniaturized LV (*Tables 1 and 2*).

Table 1: Patient characteristics

	Total	AA-MA	AA-MS	AS-MS	*P**
Perinatal variables					
Postnatal diagnosis	95/167 (56.9)	34/68 (50)	37/58 (63.8)	24/41 (58.5)	0.2
Gestational age (wk)	39.0 (32-42)	39.5 (32-42)	39.0 (35-42)	39.0 (37-42)	0.3
Prematurity	10/167 (6)	7/68 (10.3)	3/58 (5.2)	0/41 (0)	0.09
Female sex	56/167 (33.5)	29/68 (42.6)	17/58 (35.4)	10/41 (24.4)	0.1
Cardiac comorbidity	9/167 (5.4)	6/68 (8.8)	0/58 (0)	3/41 (7.3)	0.08
Extracard comorbidity	10/167 (6)	5/68 (7.4)	4/58 (6.9)	1/41 (2.4)	0.5
RAS	32/167 (19.2)	10/68 (15)	10/58 (17)	12/41 (29)	0.2
RV dysfunction	12/167 (7.2)	4/68 (6.2)	6/58 (10.3)	2/41 (4.9)	0.5
Severe TR	19/167 (11.4)	9/68 (13.2)	7/58 (12.1)	3/41 (7.3)	0.6
Norwood stage I					
Age (days)	6 (1–31)	6 (1–31)	6 (1–17)	6 (1–21)	0.8
Weight (kg)	3.4 (1.8–4.8)	3.4(1.8–4.5)	3.4(2.3–4.5)	3.3(2.4–4.8)	0.6
LPW (≤2.5 kg)	15/167 (8.9)	7/68 (10.3)	7/58 (12)	1/41 (2.4)	0.2
BT shunt	46/167 (27.5)	7/68 (10.3)	20/58 (34.5)	19/41 (46.3)	<0.0001
Mortality					
Interstage I	32/165 (19.4)	9/68 (13.2)	19/57 (33.3)	4/40 (10)	0.004
Overall operative	17/165 (10.3)	5/68 (7.4)	11/57 (19.3)	1/40 (2.5)	0.02
Interstage II	15/116 (12.9)	4/49 (8.2)	5/35 (14.3)	6/32 (18.8)	0.6
Post-TCPC	5/101 (5)	1/45 (2.2)	3/30 (10)	1/26 (3.8)	0.3
Overall	52/167 (31.1)	14/68 (20.6)	27/58 (46.6)	11/41 (26.8)	0.006
MAE					
ECMO/LVAD	26/167 (15.6)	10/68 (14.7)	12/58 (20.7)	4/41 (9.8)	0.3
PLE	5/167 (3)	3/68 (4.4)	2/58 (3.4)	0/41 (0)	0.4
Takedown Glenn/TCPC	6/133 (4.5)	2/59 (3.4)	1/38 (2.6)	3/36 (8.3)	0.4
Heart transplantation	10/167 (6)	5/68 (7.4)	2/58 (3.4)	3/41 (7.3)	0.6
Overall	69/167 (41.3)	20/68 (29.4)	34/58 (58.6)	15/41 (36.6)	0.003

Data are presented as median (range) or n/N (%). AA-MA: aortic and mitral atresia; AA-MS: aortic atresia-mitral stenosis; AS-MS: aortic and mitral stenosis; BTshunt: Blalock-Taussig shunt; ECMO: extracorporeal membrane oxygenation; LPW: low preoperative weight; LVAD: left ventricular assist device; PLE: protein-losing enteropathy; RAS: restrictive atrial septum; RV: right ventricular; TCPC: total cavopulmonary connection; TR: tricuspid regurgitation; Wk: week. *P value comparing anatomic hypoplastic left heart syndrome subtypes. *Licensed by https://creativecommons.org/licenses/by/4.0/*

Table 2: Left ventricular phenotypes related to outcome

	Globular	Miniaturized	Slit-like	*P**
Perinatal variables				
Prematurity	5/96 (5.2)	0/16 (0)	5/55 (9.1)	0.4
Female sex	24/96 (25)	5/16 (31.3)	27/55 (49.1)	0.01
Cardiac comorbidity	4/96 (4.2)	1/16 (6.3)	4/55 (7.3)	0.7
RAS	20/96 (20.8)	3/16 (18.8)	9/55 (16.4)	0.8
RV dysfunction	9/96 (9.4)	0/16 (0)	3/55 (5.5)	0.3
Severe TR	10/96 (10.4)	1/16 (6.3)	8/55 (14.5)	0.6
Anatomic HLHS subtypes				
AA-MA	13/96 (13.5)	0/16 (0)	55/55 (100)	<0.001
AA-MS	58/96 (60.4)	0/16 (0)	0/55 (0)	
AS-MS	25/96 (26)	16/16 (100)	0/55 (0)	
Norwood stage I				
LPW (≤2.5 kg)	9/96 (9.4)	0/16 (0)	6/55 (10.9)	0.4
BT shunt	36/96 (37.5)	7/16 (43.8)	3/55 (5.5)	<0.0001
Mortality				
Interstage I	27/95 (28.4)	0/15 (0)	5/55 (9.1)	0.002
Overall operative	14/95 (14.7)	0/15 (0)	3/55 (5.5)	0.08
Interstage II	10/62 (11.3)	1/13 (7.4)	4/41 (9.8)	0.5
Post-TCPC	4/52 (7.7)	0/12 (0)	1/37 (2.7)	0.4
Overall	41/96 (42.7)	1/16 (6.3)	10/55 (18.2)	0.0006
MAE				
ECMO/LVAD	18/96 (18.8)	0/16 (0)	8/55 (14.5)	0.2
PLE	2/96 (2.1)	0/16 (0)	3/55 (5.5)	0.4
Takedown Glenn/TCPC	3/68 (4.4)	1/15 (6.7)	2/50 (4)	0.9
Heart transplantation	5/96 (5.2)	0/16 (0)	5/55 (9.1)	0.4
Overall	51/96 (53.1)	2/16 (12.5)	16/55 (29.1)	0.0007

Data are presented as n/N (%). AA-MA: aortic and mitral atresia; AA-MS: aortic atresia-mitral stenosis; AS-MS: aortic and mitral stenosis; ECMO: extracorporeal membrane oxygenation; LPW: low preoperative weight; LVAD: left ventricular assist device; PLE: protein-losing enteropathy; RAS: restrictive atrial septum; RV: right ventricular; TCPC: total cavopulmonary connection; TR: tricuspid regurgitation. *Licensed by https://creativecommons.org/licenses/by/4.0/*

Univariate analyses related to adverse outcome

In the univariate analyses, perinatal and early surgical variables such as female sex, cardiac comorbidity or RAS/IAS, low preoperative weight or RV dysfunction prior to Norwood stage I, and the palliation with a BTs were associated with interstage I mortality, overall mortality, and/or the occurrence of MAE. Norwood stage I palliation with BTs was still linked to adverse outcome, when adjusted for the year of surgery ($p \leq 0.01$). The clear influence of the year of the Norwood Stage I procedure on adverse outcome in the univariate analysis was no longer present, when the cohort was divided into an early (1999-2008) and a recent (2009-2018) era. Patients with the anatomic subtype AA-MS (*Table 1 and Figure 15A and B*) or a globular LV (*Table 2, Figure 15C and D*) had the highest interstage I mortality, overall mortality and MAE.

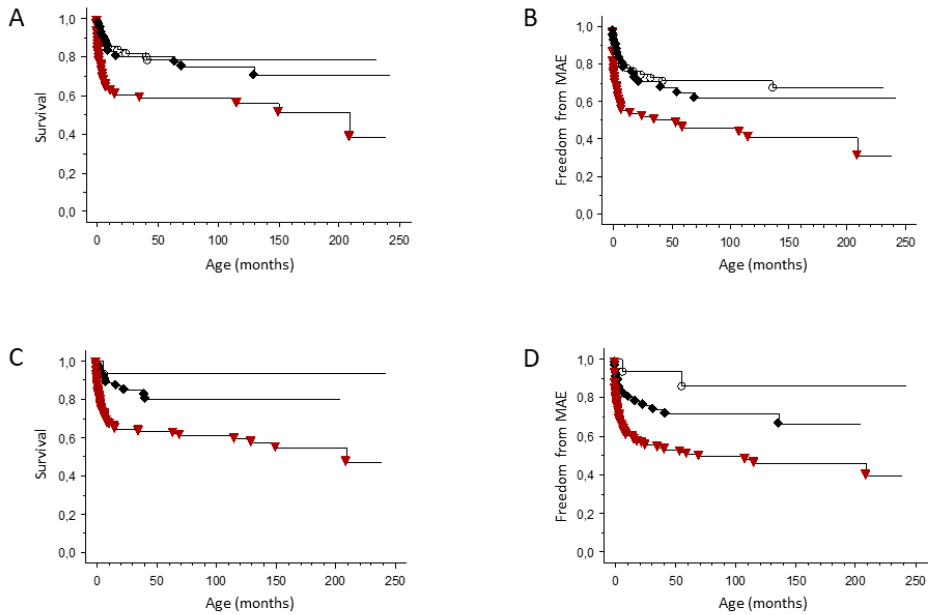

Figure 15: Impact of left ventricular morphology on adverse outcome. Kaplan-Meier analysis. **Anatomic HLHS subtypes** in relation to A) Total survival or B) MAE. Red triangle: AA-MS; black rhomb: AS-MS; black circle: AA-MA (Log-rank test: p=0.004; p=0.003, respectively). **LV phenotypes** in relation to C) Total survival or D) MAE. Red triangle: globular LV; black rhomb: slit-like LV, black circle: miniaturized LV. (Log-rank test: p=0.001; p=0.002, respectively). *Illustration reproduced from Fricke et al., JAHA 2022* [80]*, licensed by* https://creativecommons.org/licenses/by/4.0/

Multivariate analyses related to adverse outcome

Even after introducing significant perinatal variables, shunt type and year of Norwood stage I procedure in a multivariate model, AA-MS or a globular LV and

the use of a BTs were still significantly associated with interstage I and overall mortality as well as MAE. There was no interaction between AA-MS or a globular LV and shunt type in the multivariate Cox regression model (p≥0.3).

The independent association of globular LV with adverse outcome

To distinguish between the effect of globular LV and AA-MS on adverse outcome, we divided the cohort into the following three subgroups: A) patients with globular LV and with AA-MS (n=58); B) patients with globular LV in absence of AA-MS (n=38), and C) patients without both globular LV and AA-MS (n=71). The latter showed the best survival and the least MAE compared to the other two subgroups. The group with globular LV and AA-MS had the worst outcome, however, without significant differences to the group with globular LV but without AA-MS (p ≥ 0.2) (*Table 3, Figure 16 A-B*). In the multivariate Cox regression model, no interaction between the three subgroups and the shunt type was noted (p ≥ 0.3).

Table 3: Impact of globular LV in presence or absence of AA-MS on adverse outcome

	IS-I		overall		MAE	
	HR 95%	*P*	HR 95%	*P*	HR 95%	*P*
UNIVARIATE						
No glob LV/ no AA-MS vs						
Glob LV/no AA-MS	3.2 (1.1–9.9)	0.04	2.6 (1.2–5.7)	0.02	1.9 (1.0–3.8)	0.04
Glob LV/AA-MS	5.6 (2.1–15.0)	0.001	3.7 (1.8–7.4)	<0.001	2.9 (1.6–5.1)	<0.001
MULTIVARIATE						
No glob LV/ no AA-MS vs						
Glob LV/no AA-MS	3.1 (0.9–10.3)	0.06	2.6 (1.1–6.3)	0.03	2.0 (1.0–4.1)	0.07
Glob LV/AA-MS	5.1 (1.8–14.0)	0.002	3.7 (1.8–7.8)	<0.001	3.3 (1.8–6.1)	<0.001
Female sex	2.1 (1.0–4.5)	0.05	2.0 (1.1–3.7)	0.02	1.6 (1.0–2.7)	0.07
Cardiac comorbidity					3.4 (1.4–8.6)	0.009
RAS			1.8 (1.0–3.5)	0.07	2.0 (1.1–3.6)	0.02
RV dysfunction	3.3 (1.3–8.6)	0.01	2.6 (1.04–6.4)	0.04	3.0 (1.4–6.7)	0.006
LPW	5.1 (2.2–12.1)	<0.001	3.9 (1.8–8.3)	0.001	3.3 (1.7–6.6)	0.001
BT shunt	2.5 (1.1–5.7)	0.03	3.0 (1.6–5.9)	0.001	2.1 (1.2–3.8)	0.01
Year of Norwood stage I	1.0 (0.9–1.1)	0.7	1.1 (1.0–1.1)	0.8	1.0 (1.0–1.1)	0.4

Data are presented as median (range). AA-MS: aortic atresia-mitral stenosis; BT shunt: Blalock-Taussig shunt; Glob-LV: globular left ventricle; HR: hazard ratio; IS-I: interstage I; LPW: low preoperative weight; RAS: restrictive atrial septum; RV: right ventricular. *L.b.* https://creativecommons.org/licenses/by/4.0/

BTs palliation in patients belonging to morphological high risk groups

BTs palliation in patients with either the anatomic subtype AA-MS or a globular LV phenotype was associated with increased overall mortality compared to those with a Norwood stage I Sano palliation (*Figure 16 C and D*), even when corrected for the year of surgery ($p \leq 0.05$).

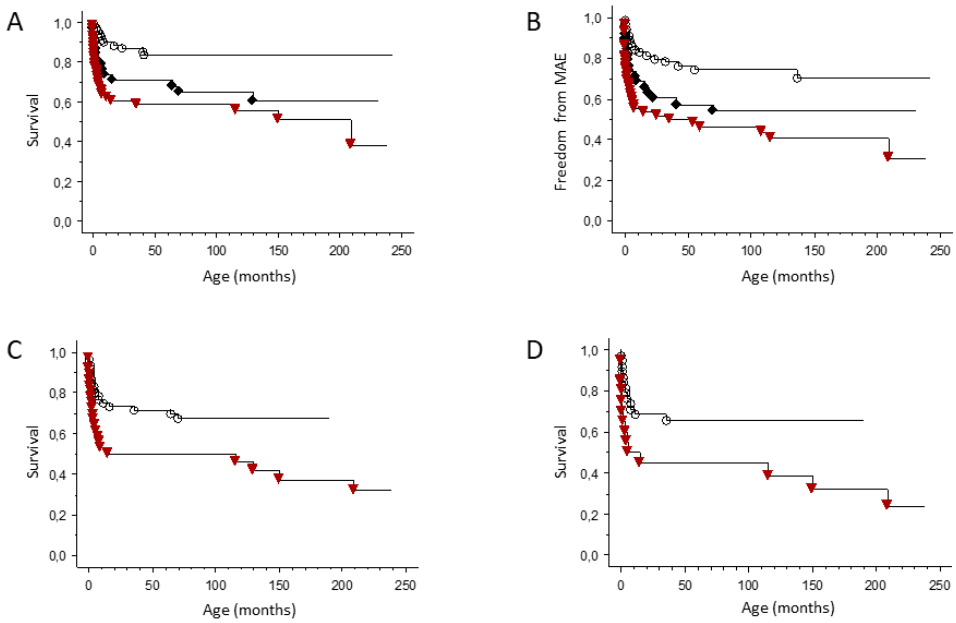

Figure 16: Impact of combined left ventricular morphology on adverse outcome and impact of choice of shunt in morphological risk groups on adverse outcome. Kaplan-Meier curves are provided. **Globular LV with and without AA-MS** in relation to A) Total survival and B) MAE. Red triangle: globular left ventricle with AA-MS, black rhomb: globular left ventricle without AA-MS, black circle: all other left ventricular phonotypes and anatomic HLHS subtypes (Log-rank test: p=0.0006; p= 0.0009, respectively). **Choice of shunt** in patients with C) AA-MS or D) Globular LV in relation to total survival. Red triangle: palliation with Blalock-Taussig shunt, black circle: palliation with Sano shunt (Log-rank test: p=0.03, p=0.002, respectively). *Illustration reproduced from Fricke et al., JAHA 2022* [80]*, licensed by* https://creativecommons.org/licenses/by/4.0/

Perinatal risk factors with significant impact on morbidity and mortality are shown in *Figure 17*.

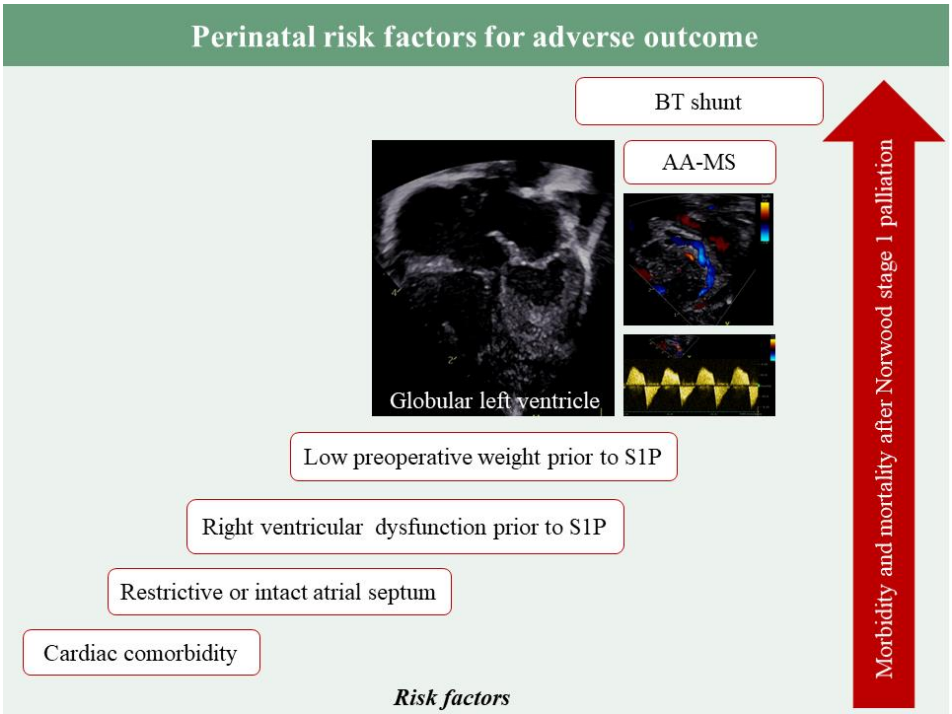

Figure 17: Impact of perinatal risk factors on adverse outcome. AA-MS: aortic atresia-mitral stenosis; BT shunt: modified Blalock-Taussig shunt; S1P: Norwood stage I palliation. *Unpublished illustration by Dr. Katrin Fricke*.

Paper III

Magnetic Resonance Imaging of the Descending Aorta in Suspected Left-Sided Cardiac Obstructions

The aim of this fetal phase-contrast CMR study was to compare Doppler ultrasound-based flow measurements in the DAo and UV in fetuses with suspected left heart obstructions with and without the need for a neonatal intervention and in healthy controls. A secondary aim was to improve the fetal diagnosis of CoA by adding fetal CMR flow measurements in the DAo and UV to the fetal echocardiographic variables, highly predictive of CoA in our retrospective study (Paper I).

Study population and patient characteristics

Of the 54 included fetuses with suspected left heart obstructions and healthy controls, 3 had to be excluded due to suboptimal DAo and UV flow studies. Of the remaining 51 fetuses, 30 had suspected CoA, 11 HLHS, 5 cAS and a further 5 were healthy controls.

Fetal CMR was performed in late pregnancy (median gestational age 35.5 (3.5) days) with an estimated fetal weight of 2720 (1157) grams. Seven fetuses had FGR at the time of the fetal CMR.

All fetuses survived to delivery, whereas six infants with HLHS or cAS died during follow-up, the majority (n=5) in the neonatal period.

Neonatal surgery for left heart obstructions was performed in all neonates with confirmed (true) CoA (n=8; 27%), all cAS (n=5) and HLHS, except for one infant with HLHS and IAS, who was managed according to comfort care (n=10). One additional neonate with borderline left heart structures underwent surgical ductal closure, without requiring further intervention during follow-up.

Fetal CMR flow measurements related to neonatal outcome

The interobserver agreement for fetal CMR-derived DAo flow measurements was excellent with an ICC of 0.95 (0.92–0.97).

Fetuses with suspected left heart obstructions with or without requiring neonatal intervention

No significant difference in DAo or UV flow was found in fetuses with left heart obstructions with and without requiring neonatal intervention and in healthy controls.

Retrograde systolic isthmic fetal echo flow related to fetal CMR flows and outcome

Our study showed, that retrograde systolic isthmic flow on fetal echo, used as a possible indirect marker of severe left-sided outflow tract obstruction, was linked to reduced total DAo and UV flow, net DAo flow and changes in DAo downslope (*Figure 18*, *Table 4*). Retrograde isthmic flow, seen in all fetuses with HLHS (n=11), 80% with cAS (n=4), 25% with true CoA (n=2) and 9% with false positive CoA (n=2), was associated with the need for cardiac surgery in the neonatal period ($p<0.001$), as well as one-year mortality ($p=0.02$).

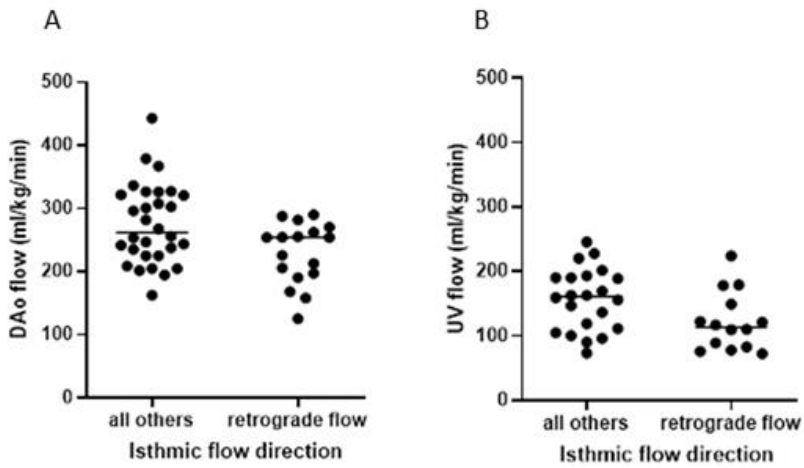

Figure 18: Fetal blood flow in the A) DAo and B) UV with and without retrograde systolic isthmic flow. Solid black line refers to the median. *Illustration reproduced from Fricke et al., Frontiers in Cardiovascular Medicine. 2023* [100]*, licensed by* https://creativecommons.org/licenses/by/4.0/

Table 4: Fetuses with retrograde systolic isthmic flow versus all others

	All others	n	Retrograde flow	n	*P*
Fetal cardiac examination					
Gestational age (weeks)	35.1 [3.9]	32	36.6 [3.9]	19	0.09
Estimated weight (grams)	2627 [1032]	32	2820 [1076]	19	0.3
Fetal growth restriction	4 (13)	32	3 (16)	19	1
Associated cardiac anomalies					
L-SVC	2 (7)	27	0 (0)	19	0.3
VSD	5 (19)	27	2 (11)	19	0.6
Atrial septal aneurysm	11 (41)	27	0 (0)	19	0.001
RAS	1 (4)	27	6 (32)	19	0.02
Fetal echocardiogram					
Foramen ovale flow					
Right-to-left	12 (44)	27	2 (11)	19	<0.001
Bidirectional	14 (52)		5 (26)		
Left-to-right	0 (0)		9 (47)		
None	1 (4)		3 (16)		
Fetal CMR					
Descending aortic flow					
Total flow (ml/kg/min)	261 [97]	30	253 [72]	17	0.035
Minimum flow (ml/kg/s)	0.9 [1.3]	30	0.5 [1.1]	17	0.09
Upslope/net flow (ml/s)	0.032 [0.1]	30	0.038 [0.01]	17	0.2
Downslope/net flow (ml/s)	-0.016 [0.01]	30	-0.021 [0.01]	17	0.03
Net flow (ml/kg)	1.3 [0.4]	30	0.8 [0.3]	17	0.03
Total UV flow (ml/kg/min)	161 [81]	22	113 [75]	14	0.04
DAo/UV flow	1.8 [0.7]	20	2.2 [0.7]	12	0.17
Postpartum outcome					
Gestational age (weeks)	39.6 [1.7]	32	39.1 [2.2]	19	0.7
Neonatal cardiac operation	7 (22)	32	17 (89)	19	<0.001
Neonatal death	1 (3)*	32	4 (21)	19	0.058
One-year mortality	1 (3)*	32	5 (26)	19	0.02

Data are presented as median [IQR] or n/N (%). DAo: descending aorta; L-SVC: persistent left superior vena cava; RAS: restrictive atrial septum; UV: umbilical vein, *: fetus with critical aortic stenosis dying of its metabolic disease. *Licensed by https://creativecommons.org/licenses/by/4.0/*

DAo and UV flow in fetuses with HLHS or cAS

Fetuses with HLHS or cAS showed signs of reduced peak, net and total DAo flow, but no difference in flow pattern compared to all other fetuses, including healthy controls. The coexistence of RAS/IAS did not further alter DAo or UV flow ($p>0.3$), but was associated with both neonatal and one-year mortality ($p \leq 0.04$).

Differences in fetal echocardiographic and CMR-derived variables between fetuses with true and false positive CoA

As already shown in our retrospective fetal echocardiography study (Paper I), ratios including the I/D(3VT), I/D3VTxMV/TV and CSAI, flow anomalies across the atrial septum and the presence of a posterior shelf were significantly associated with true CoA (*Figure 19A*) [92]. Associated minor CHDs were equally distributed between the groups, but one of the pitfalls of our study was that fetuses with true CoA were studied in earlier gestation compared to those with false positive CoA. No significant difference in fetal CMR-derived DAo or UV flows was found between fetuses with or without true CoA. However, a trend towards increased maximum DAo velocity was observed in those with true CoA (*Figure 19B*). Combining significant fetal echocardiographic variables with fetal CMR flow data in a multivariate regression analysis did not improve the fetal diagnosis of CoA ($p \geq 0.2$).

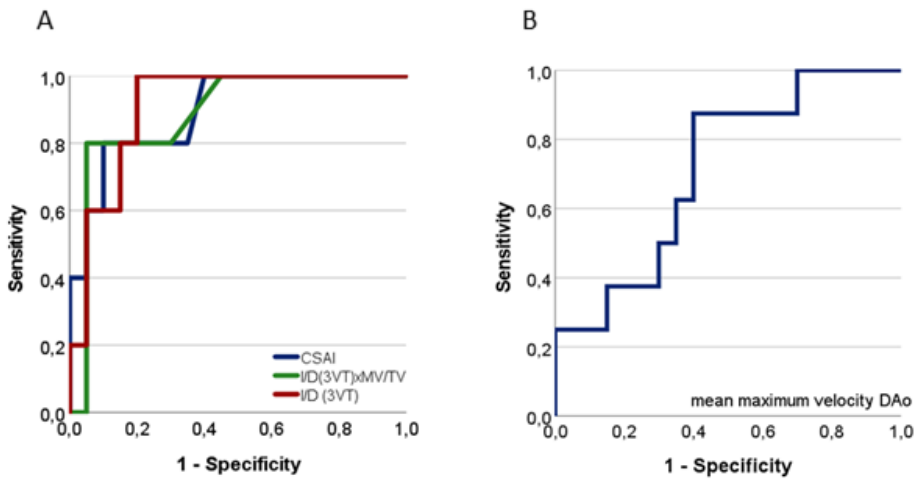

Figure 19: ROC curves relating fetal CMR and echo-derived variables to the outcome of true CoA.
A) Fetal echocardiographic variables related to the outcome of true CoA.
CSAI: carotid-subclavian artery index, (AUC = 0.89; p = 0.007);
I/D(3VT): isthmus-to-duct ratio in the 3VT view (AUC = 0.91; p = 0.005);
I/D(3VT)xMV/TV: product of I/D(3VT) with the mitral-to-tricuspid valve ratio (AUC = 0.89; p = 0.009).
B) Fetal CMR-derived mean maximum velocity in the DAo related to the outcome of true CoA (AUC 0.71; p = 0.08). *Illustration reproduced from Fricke et al., Frontiers in Cardiovascular Medicine 2023 [100], licensed by* https://creativecommons.org/licenses/by/4.0/

5) RAS in fetuses with suspected CoA in relation to DAo and UV flow

The presence of RAS in both fetuses with true CoA (n=2) and false positive CoA (n=2) was associated with reduced total DAo and UV flows, minimum and net DAo flows, as well as changes in DAo upslope and downslope. In addition, higher maximum DAo flow velocities and DAo-to-UV flow ratios were observed in fetuses with RAS. Three out of four fetuses with suspected CoA and RAS had retrograde systolic isthmic flow. None of them had FGR.

Paper IV

Three-dimensional Arch Geometry and Blood Flow in Neonates After Surgical Repair for Aortic Coarctation

The aim of this prospective MRI study was to assess the geometry and flow pattern in the distal aortic arch early after neonatal CoA repair, and to compare these parameters between neonates who developed re-CoA early after repair and those who did not.

Study population and patient characteristics

Complete MRI data were available for 28 neonates after the exclusion of 8 cases. Median gestational age and weight were 39.6 (2.2) weeks and 3270 (739) grams, respectively. Associated CHDs such as VSD (n=14), BAV (n=19) or a marked aortic arch hypoplasia (n=20) were seen in the majority of the included neonates.

Surgical data

Neonatal CoA repair was performed at a median age of 9 (11) days. Lateral thoracotomy was used in 12 (43%) neonates, including 4 with end-to-end, 7 with extended end-to-end and 1 with end-to-side anastomosis. The remaining neonates required median sternotomy, either because of marked aortic arch hypoplasia and/or concomitant VSD in need of neonatal repair (n=8). Surgical techniques included end-to-side anastomosis (n=5) or aortic arch repair with autologous patch material (n=11). Four neonates had a bovine aortic arch.

MRI assessment

MRI was performed at a median age of 16 (9) days and a weight of 3410 (990) grams. Of the 28 patients included, 17 had a roman, 9 had a crenel and 2 had a gothic aortic arch configuration. The type of neonatal CoA repair was not associated with postoperative arch shape (p=0.2).

Relationship between aortic arch shape, 3D angles and flow pattern

Infants with a crenel aortic arch, followed by roman and gothic arches, had the largest angle between the ascending and descending aorta (p=0.02) and the largest distance between the first and last branching points (p=0.03). In addition, patients with a gothic arch had more peak vortical flow than those with the other two arch shapes (p=0.03). Helical flow did not differ between the three subgroups.

As the angle between the ascending and descending aorta increased, a trend towards more left-handed diastolic flow was noted (Pearson´s correlation coefficient 0.362; p=0.056). With increasing anteroposterior arch angulation, more peak and diastolic vortical flow and less left-handed helical flow were observed (*Figure 20 A and B*).

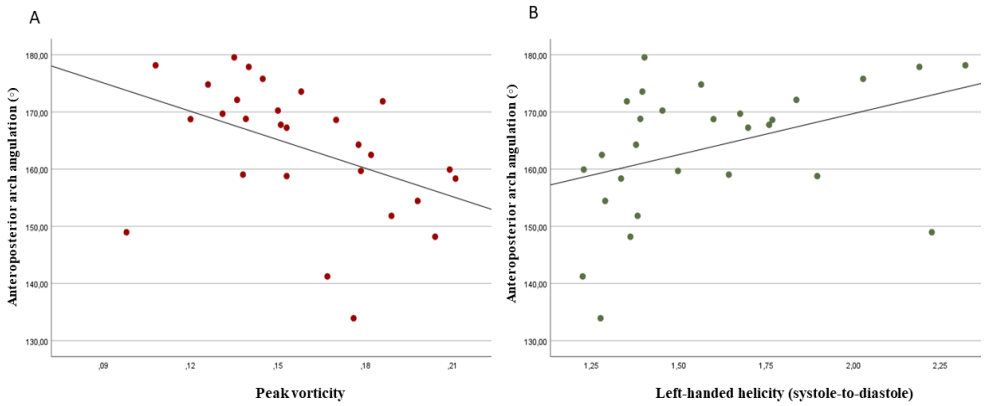

Figure 20: Relationship between anteroposterior arch angulation and flow pattern in the distal aortic arch. A) Peak vorticity (Pearson´s correlation coefficient -0.438; p=0.02) B) Left-handed helicity (Pearson´s correlation coefficient 0.396; p= 0.03). *Unpublished illustration by Fricke et al.*

As the angle between the ascending aorta and the brachiocephalic artery increased, peak right-handed helicity increased, and as the angle between the proximal aortic arch and the left common carotid artery increased, diastolic right-handed helical flow decreased (*Figure 21A and B*).

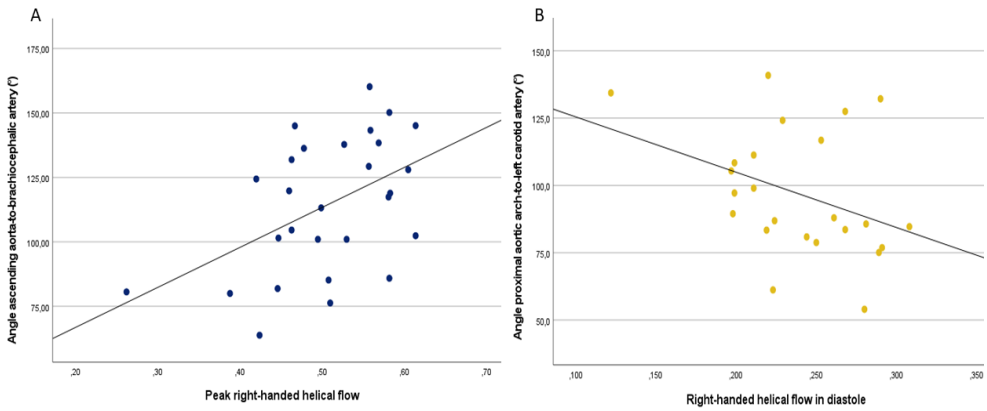

Figure 21: Relationship between the angle between A) The ascending aorta and the brachiocephalic artery to right-handed peak helicity (Pearson´s correlation coefficient 0.475, p=0.01), B) The angle between the proximal aortic arch and the left common carotid artery and right-handed diastolic flow (Pearson´s correlation coefficient -0.376; p=0.07). *Unpublished illustration by Fricke et al.*

Relationship between calibre change and flow pattern

The postoperative calibre change between the distal ascending aorta just before the origin of the brachiocephalic artery and the distal aortic arch just before the origin of the left subclavian artery was negatively associated with vorticity (peak: Pearson´s correlation coefficient -0.35, p=0.015; diastolic: Pearson´s correlation coefficient -0.39, p=0.04), and right-handed helicity (peak: Pearson´s correlation coefficient -0.46, p=0.01; systolic: Pearson´s correlation coefficient -0.38, p=0.04).

Recurrent coarctation (re-CoA)

Re-CoA occurred in four patients at a median age of 3.5 (1.2) months.

Patient characteristics such as gestational age, birth weight, sex and the presence of associated VSD and BAV or a bovine arch were equally distributed between patients with and without the formation re-CoA.

Surgical technique in relation to re-CoA

Surgical technique was associated with re-CoA, with all of these patients having undergone a lateral thoracotomy with either end-to-end or extended end-to-end anastomosis. Young age (<15 days) or low preoperative weight (≤2.5 kg) at neonatal surgery were not associated with re-CoA.

Aortic arch geometry and flow pattern in relation to re-CoA

All patients with re-CoA had a crenel arch configuration after neonatal CoA repair (*Table 5*). A trend towards a smaller angle between the ascending aorta and the brachiocephalic artery, and a smaller angle between the proximal aortic arch and the left common carotid artery were seen in patients with re-CoA (*Table 5, Figure 22 A and B)*. The change in aortic arch calibre was greater in patients with re-CoA than in those who did not develop re-CoA (*Table 5, Figure 23A and B*).

Patients with re-CoA had increased left-handed systolic helical flow and right-handed diastolic helical flow, and a trend towards less vortical flow (*Table 5, Figure 24 A and B).*

Table 5: MRI-derived variables related to outcome re-CoA

	No re-CoA	n	Re-CoA	n	*P*
Aortic arch geometry					
Aortic arch shape Roman Gothic Crenel	 17 (71) 2 (8) 5 (21)	24	 0 (0) 0 (0) 4 (100)	4	0.007
3D angles **(˚)**					
AAo-to-DAo	110.8 [13.3]	24	119.4 [15.3]	4	0.15
Anteroposterior angulation	165.8 [16.6]	24	168.8 [12.0]	4	0.6
AAo-to-brachiocephalic artery	121.7 [37.1]	24	90.5 [37.9]	4	0.06
Proximal arch-to-LCCA	97.2 [37.0]	21	75.1 [-]	3	0.04
Distance first-to-last branching points (mm)	7.31 [6.98]	24	12.43 [11.18]	4	0.2
Arch angle-to-distance	15.11[15.88]	24	9.06 [94.64]	4	0.3
Calibre change					
AAo-to-proximal aortic arch	0.86 [0.76]	21	1.85 [-]	3	0.03
AAo-to-distal aortic arch	1.01 [0.94]	24	2.19 [2.42]	4	0.03
AAo-to-isthmus	1.50 [0.89]	24	1.74 [1.53]	4	0.5
Helicity and vorticity					
Systolic right-handed helicity	0.453 [0.095]	24	0.441 [0.095]	4	0.8
Diastolic right-handed helicity	0.227 [0.061]	24	0.281 [0.015]	4	0.018
Right-handed helicity (s-to-d)	1.993 [0.56]	24	1.548 [0.41]	4	0.018
Mean left-handed helicity	0.269 [0.080]	24	0.313 [0.052]	4	0.06
Systolic left-handed helicity	0.337 [0.101]	24	0.394 [0.060]	4	0.045
Peak vorticity	0.162 [0.047]	24	0.133 [0.028]	4	0.07
Mean vorticity	0.117 [0.026]	24	0.098 [0.022]	4	0.07
Diastolic vorticity	0.127 [0.025]	24	0.106 [0.020]	4	0.05

Data are presented as median [IQR] or n/N (%). AAo: ascending aorta, DAo: descending aorta; LCCA: left common carotid artery; LSA: left subclavian artery. S-to-d: systole-to-diastole. *Unpublished data by Fricke et al.*

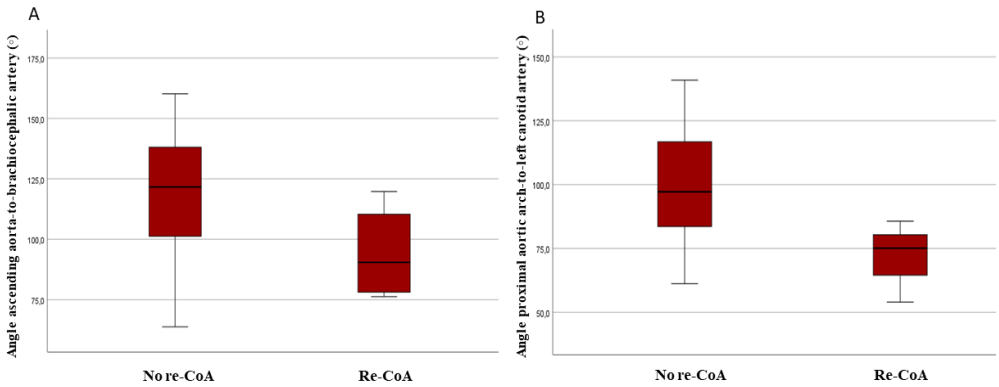

Figure 22: Three-D aortic arch angles related to outcome re-CoA. A) Angle between the ascending aorta and brachiocephalic artery (p=0.06). B) Angle between the proximal aortic arch and left common carotid artery (p=0.04). *Unpublished illustration by Fricke et al.*

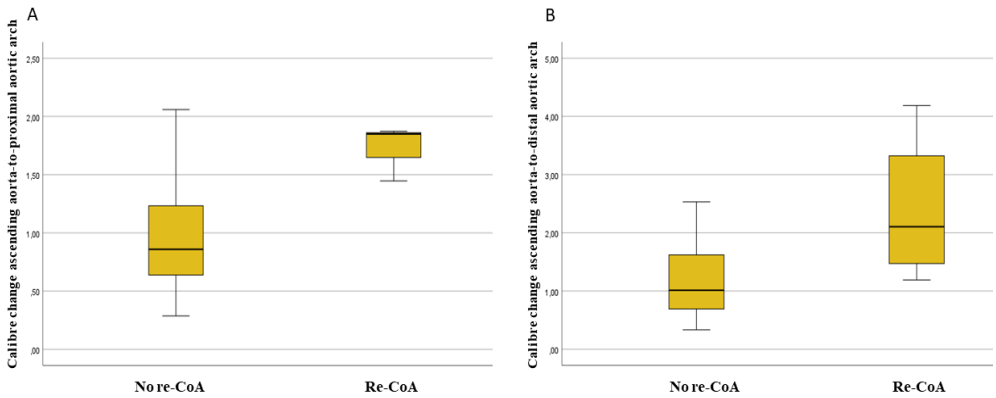

Figure 23: Aortic arch calibre change in relation to outcome re-CoA. A) Ascending aorta-to-proximal aortic arch (p=0.03). B) Ascending aorta-to-distal aortic arch (p=0.03). *Unpublished illustration by Fricke et al.*

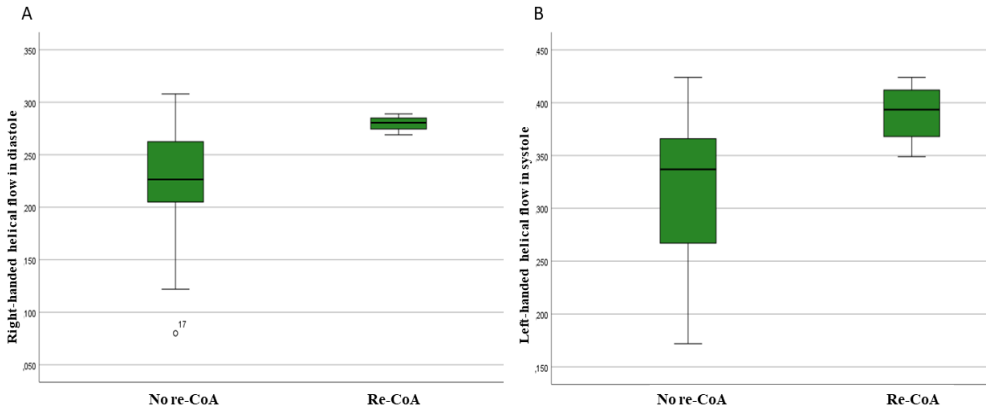

Figure 24: Flow pattern in the distal aortic arch in relation to outcome re-CoA. A) Right-handed helical flow in diastole (p=0.02). B) Left-handed helical flow in systole (p=0.045). *Unpublished illustration by Fricke et al.*

Pre-discharge clinical data in relation to outcome re-CoA

No difference in the systolic blood pressure gradient between arm and leg, but in echocardiographic isthmic flow velocity, was noted after neonatal CoA surgery before discharge in those patients who later developed re-CoA (p=0.04).

Discussion

Paper I

In this retrospective fetal echocardiography study, we found that CoA could be predicted with high accuracy using the CSAI or I/D3VTxMV/TV.

Ratios

A number of ratios between the right and left heart structures have been proposed as reliable predictors of true CoA in previous studies [9,12-15].

CSAI and I/D3VTxMV/TV were the best predictors of true CoA in our study.

Initially, the use of CSAI was suggested for patients with an uncertain neonatal diagnosis of CoA in the presence of a persistent arterial duct [28]. Subsequently, this index was applied in two fetal echocardiography studies, but these had small sample sizes and did not provide cut-off points with corresponding sensitivity and specificity, making its use in a clinical setting difficult [101,102]. Our study was the first to demonstrate the CSAI as a superior predictor of true CoA. However, it requires a sagittal aortic arch view, which can be difficult to obtain in late gestation, when echo windows are often poor.

The I/D3VTxMV/TV is an appealing alternative with the advantage of incorporating both the ventricular and isthmic-to-duct disproportion without the need for a sagittal aortic arch view.

Thus, both CSAI and I/D3VTxMV/TV were able to predict true CoA with high accuracy and will be further investigated in a nationwide prospective fetal CoA study.

Another finding of this study was that ratios were superior to Z-scores in predicting CoA, probably because measurement inaccuracies are less important when ratios are used. In addition, Z-scores do not take into account fetal weight and size, which can lead to incorrect conclusions for fetuses, small or large for gestational age.

Z-scores

Fetuses with true CoA had significantly smaller left heart structures and lower corresponding Z-scores than those with false positive CoA. Of these, Z-scores of the MV annulus, ascending aorta and aortic isthmus in the sagittal or 3VT views were most predictive, as already shown in previous studies [9,16,101,103].

In the literature, only one Z-score data set per anatomic structure is typically used, usually Pasquini *et al.* for isthmic and ductal diameters and Schneider *et al*. for intracardiac structures [89,90]. In our study, we used different Z-score data sets and found significant differences for measurements of the same anatomic structures [87-90]. The small number of fetuses included in the different Z-score data sets may explain the observed discrepancies. It is therefore extremely important to interpret the calculated Z-scores with caution in order to avoid erroneous conclusions.

Qualitative variables

The association of qualitative variables such as the presence of borderline left heart structures, aortic arch hypoplasia or a posterior shelf as well as flow anomalies across the atrial septum or aortic arch with postpartum outcome has been studied before and was also found in our study [9,16,17,101,103]. However, it must be recognised, that subjective qualitative assessment depends on the examiner and is inferior to quantitative measurements. As our study also showed, the specificity of the observed flow anomalies was low, which may cause unwarranted anxiety in expectant parents, if this finding leads to the false conclusion, that CoA, or even worse, postnatal univentricular outcome, may be imminent.

Paper II

This nationwide retrospective Swedish study of patients with HLHS demonstrated an independent association of the anatomic subtype AA-MS and a globular left ventricle with adverse outcome, especially when a BTs was used as part of their Norwood stage I palliation.

Association of AA-MS with adverse outcome

Previous studies have reported an association between AA-MS and mortality [75-77,104,105]. This finding has been attributed to coronary anomalies such as coronary stenosis or ventriculo-coronary connections, probably due to high LV intraventricular pressure, which may cause ventricular ischaemia and sudden death [104,105]. However, two previous autopsy and angiography studies have demonstrated ventriculo-coronary connections in only a fraction of patients with AA-MS [106,107], which therefore cannot fully explain the high mortality rate in this subgroup. In contrast, other studies, including the Single Ventricle Reconstruction (SVR) trial, have not found an association between AA-MS and mortality, probably due to differences in neonatal surgical approach and perioperative care between centres [104,107,108].

Association between LV phenotype, anatomic HLHS subtype and outcome

The association of a globular LV and the anatomic subtypes AA-MS and AS-MS with critical aortic stenosis has been described before [78,79]. However, in our study, a globular LV was also found in individual cases with AA-MA, probably due to the progression from MS to MA in fetal life, as suggested by a previous study [109].

An interesting new finding of our study was the association of globular LV with adverse outcome, irrespective of the concomitant presence of AA-MS. We therefore hypothesized that LV size, shape and function and their effect on RV function, rather than the presence of coronary anomalies, may explain, at least in part, the association with morbidity and mortality. The impact of a remnant LV on RV performance and outcome has been investigated in previous studies, but with conflicting results [82,83,108,110]. The majority of these studies divided their cohort into two LV phenotypes, those with an absent LV (corresponding to a slit-like LV) and those with a remnant LV (corresponding to a globular or miniaturized LV) [82,83,108,110]. In the presence of a remnant LV, basal intraventricular septal strain was reduced in two studies [82,83] and associated with adverse outcome [83]. The SVR trial found improved RV diastolic function in patients with an absent LV, but no effect on outcome related to LV size or function [108]. One reason for these conflicting

results may be that the group with remnant LV included patients with both a miniaturized LV (associated with the best outcome in our study) and a globular LV (associated with the worst outcome in our study). Other studies have found an association between ventricular septal hypertrophy and a larger LV size with adverse outcome [81,84]. Interestingly, one study associated a "bulging RV" caused by apicolateral LV hypertrophy (which best fits the globular LV phenotype) with RV dysfunction and adverse outcome [109]. It is reasonable to assume, that the negative impact of the globular LV phenotype on outcome is 1) caused by a negative ventricular-ventricular interaction and 2) further exacerbated by the concomitant occurrence of coronary anomalies in patients with a globular LV and AA-MS. In contrast, a miniaturized LV may contribute to RV ejection through a positive effect on ventricular septal function [109].

Choice of Norwood stage I shunt in morphologically high risk groups

Our study demonstrated improved early and overall outcomes when a Sano shunt was used as part of the Norwood stage I palliation, particularly in the first year of life. Improved early, but not overall, survival with the use of Sano shunts has been reported previously and may be partly related to more stable coronary perfusion compared to the use of BT shunts [60,111-114]. However, disadvantages of the Norwood stage I Sano palliation may include a higher rate of shunt re-interventions and RV scarring with subsequent RV dysfunction and arrhythmias [60,115,116].

Another important finding of our study was that patients with the anatomic HLHS subtype AA-MS or a globular LV exhibited increased overall mortality, when palliated with a BTs. Increased intermediate mortality has previously been reported with BTs palliation in patients with a single right ventricle and aortic atresia [117]. However, in patients with AA-MS, no difference in survival was observed, in relation to the type of shunt used at Norwood stage I, probably due to the small sample size of those who received a BTs [77,118].

Our finding of increased overall mortality in patients with a globular LV or AA-MS palliated with a BTs may derive from the coronary steel phenomenon induced by the BTs palliation on top of the negative impact of a globular LV and/or coronary anomalies on systemic right ventricular function.

Paper III

Adding fetal CMR flow measurements in the DAo and UV did not aid to discriminate between fetuses with suspected left heart obstructions with or without the need for neonatal cardiac intervention. However, those with retrograde systolic isthmic flow, including fetuses with severe outflow tract obstructions such as HLHS and cAS, and those with suspected CoA and RAS, had significantly reduced DAo and UV flows.

Lloyd *et al.* demonstrated that reduced flow in the ascending aorta in combination with changes in the aortic arch configuration were predictive of true CoA [21]. However, the perpendicular visualization of the ascending aorta in the fetal thorax in order to reliably measure flow is challenging. For this reason, we chose the DAo as an alternative for reliable flow measurements [27].

Differences in DAo and UV flow between different groups

Fetuses with suspected left heart obstructions with or without needing neonatal cardiac intervention

The lack of differences in DAo flow between fetuses with and without the need for neonatal cardiac intervention is most likely due to differences in the flow physiology of the different subgroups. In less severe outflow tract obstructions, the decrease in flow through the left side of the heart may be compensated for by increased right-sided cardiac flow, resulting in the same amount of DAo flow. However, in severe outflow tract obstructions, retrograde systolic isthmic flow may occur, resulting in reduced combined cardiac output and consequently reduced DAo flow.

Retrograde systolic isthmic flow related to type of CHD, CMR-derived flows and outcome

Retrograde systolic isthmic flow on fetal echo was encountered almost exclusively in fetuses with severe left heart obstructions such as HLHS and cAS, but also in isolated cases of suspected CoA with or without RAS, which is consistent with the literature [119,120]. Reduced combined cardiac output has been reported in fetuses with severe left heart obstructions in a fetal CMR study [121]. In addition, abnormal RV function has been observed in fetuses with HLHS and cAS with evolving HLHS, most pronounced in the latter [122,123]. In our study, three out of five fetuses with cAS had RV dysfunction due to a negative ventricular-ventricular interaction that impeded right ventricular filling.

Thus, it is likely that combined left and right ventricular dysfunction in fetuses with HLHS or cAS leads to reduced combined CO and ultimately reduced DAo flow.

The four fetuses with suspected CoA (two with true CoA and two false positives) and retrograde systolic isthmic flow, had either markedly underdeveloped left heart structures and/or RAS. The presence of RAS in fetuses with suspected CoA was associated with reduced DAo and UV flows in our study.

True CoA versus false positives

Fetal echocardiographic ratios identified in our previous retrospective fetal echocardiography study, but not fetal CMR flow parameters, were predictive of true CoA [92]. A pitfall of this study was, that the gestational age of fetuses with and without true CoA at the time of fetal CMR examination differed significantly, which may have affected flow.

A recent fetal CMR study observed negative mean aortic isthmic flows in fetuses with true CoA, which were not measured but calculated by subtracting SVC from ascending aortic flows [21]. Our study could not demonstrate differences in isthmic flow direction between fetuses with and without true CoA. This is in agreement with previous studies that found low sensitivity and specificity for bidirectional or retrograde isthmic flow in predicting true CoA [8,124,125]. It should be noted that the definitive narrowing of the aortic isthmus often occurs postpartum when the arterial duct closes [121]. In these cases, no obvious flow anomalies in the aortic isthmus may be present in fetal life.

The lack of differences in DAo flow between fetuses with true and false positive CoA derives probably from a more pronounced compensatory increase in flow across the right side of the heart in fetuses with true COA compared to false positives. Subsequently, the same amount of DAo flow would be expected in both groups.

Paper IV

This study was the first to investigate 3D aortic arch geometry and its relationship with flow pattern in the distal aortic arch in neonates after CoA repair. Such studies may contribute to a better understanding of the formation of re-CoA in the first year of life. Our findings indicated an association between aortic arch geometry, distal aortic arch flow pattern and re-CoA, but the number of infants who developed re-CoA was very small. Whether the identified differences could account for the development of re-CoA needs further investigation.

In this study, we used a 3D model of the aortic arch, which may provide a more accurate assessment of aortic arch geometry compared with previous studies. Furthermore, we quantified the helical and vortical flow in the aortic arch using the 3D vector matching method developed by Heiberg *et al.* [99], in contrast to several previous studies that used a qualitative approach [126-129].

Aortic arch geometry and flow pattern after neonatal CoA repair

Aortic arch geometry

Three different postoperative aortic arch shapes including a roman, a crenel, and a gothic arch have been described in the literature [40]. A gothic arch has been linked to a higher risk of systemic hypertension, increased LV mass and decreased left ventricular function compared to the other two aortic arch shapes [130-133].

Previous studies have focused on the angles between different segments of the aortic arch and between the ascending and descending aorta [40,54,134]. However, a more complex model of the aortic arch morphology may be required to assess its influence on hemodynamics [135]. The 3D angle analysis model used in our study included not only the previously mentioned geometric variables, but also the anteroposterior arch angulation and the angles between the arch and the branching points of the first two head-neck vessels (*Figure 12*).

Flow pattern in the distal aortic arch

The application of 4D flow in the aortic arch is feasible in neonates, as already demonstrated in a recent study from our centre [98]. Four-D flow may aid to visualize changes in the aortic arch flow pattern, including helical and vortical flow [126-128,136]. In contrast to most previous studies, we quantitatively assessed changes in flow pattern using the 3D vector matching method proposed by Heiberg *et al.* [99]. The use of quantitative measurement methods may lead to more reliable and comparable results regarding helicity and vorticity.

In healthy adults with a left-sided aortic arch, dominant right-handed systolic arch helicity and right-handed diastolic helicity in the DAo are common findings (Lorenz *et al.,* 2011). Frydrychowicz *et al*. found aortic arch helicity, more often right-handed, in about 60% of healthy adults, especially when the arch was normally configured (roman and crooked shape) [126]. Only 10% of healthy grown-ups exhibited a vortical flow pattern in the aortic arch. With age, right-handed helicity may decrease or even change to left-handed helicity with an increase in vorticity. One reason for this observation may be the loss of elasticity of the aortic wall [126]. In agreement with these two studies, right-handed helicity was the dominant flow pattern in the distal aortic arch whereas vortical flow was rare in our cohort.

Relationship between aortic arch shape, 3D angles and flow pattern

Infants with a crenel arch had larger angles between the ascending and descending aorta and a greater distance between the first and last aortic arch branching points. Despite the pronounced peak vortical flow in infants with a gothic arch, no significant difference in flow pattern was found between the three groups. This may change with age, as healthy adults with gothic or crenel arches have less right-handed helical and more vortical flow [126]. Similar to our study, Quail *et al.* found an association between subjective identification of a gothic arch and arch angulation, but not hemodynamics, in adults after CoA repair in the first year of life [135]. This may suggest that qualitatively assessed arch shape has little influence on the flow pattern in the distal aortic arch.

In our study, an increase in vortical and decrease in left-handed helical flow was noted with increasing anteroposterior angulation of the aortic arch. To the best of our knowledge, this finding has not been described before. One could speculate that with increasing anteroposterior arch angulation, changes in the flow pattern in the distal aortic arch may occur, with possible clinical implications. However, this needs to be investigated in future studies.

Other findings not previously reported were the association between 1) a larger angle between the ascending aorta and the brachiocephalic artery with more peak right-handed helical flow, and 2) the association between a larger angle between the proximal aortic arch and the left common carotid artery with less diastolic right-handed helical flow. As mentioned above, further work is needed to understand the relevance of these findings in the clinical setting.

Relationship between calibre change and flow pattern

A smaller distal arch compared to the distal ascending aorta was associated with less vortical flow and less right-handed helical flow. This may suggest that a wider distal arch, typically found after arch reconstruction with patch, allows for more vortical and helical flow. Right-handed helical flow is the predominant flow pattern in the aortic arch in healthy adults (Lorenz *et al*., 2011) and we suspect that it is less common in patients with calibre mismatch and a smaller arch following neonatal

CoA repair, as helical flow cannot continue undisturbed in the narrow aortic arch. Consistent with our findings, Quail *et al*. found an association between a larger ascending aorta and a smaller aortic arch and descending aorta with flow anomalies [135].

Variables in relation to outcome re-CoA

The re-CoA rates observed in our study were consistent with those reported in the literature [41,42,53,137].

Coexistence of minor CHDs and their association with re-CoA

In agreement with earlier studies, the coexistence of minor CHDs such as BAV or VSD was not predictive of re-CoA [43,49,50]. However, we did not find an association between a bovine arch and re-CoA [138], which could be explained by the small number of cases with a bovine arch in our study.

Surgical data in relation to re-CoA

Simple, neonatal CoA is usually repaired by an end-to-end or extended end-to-end anastomosis via lateral thoracotomy [29]. Extended end-to-end anastomosis tends to have a lower risk of re-CoA [31,44-46], probably because the distal arch is being enlarged as part of the operation. Though, the majority of our patients required a more extensive surgical approach via median sternotomy due to marked aortic arch hypoplasia and/or concomitant VSD in need of neonatal repair. None of these patients developed re-CoA within the first year, which is consistent with previous studies reporting a lower risk of re-CoA in infants who underwent end-to-side or aortic arch repair with autologous patch material via median sternotomy [32,47,48]. In our study, none of the patients with median sternotomy had residual, postoperative hypoplasia of the ascending aorta and transverse aortic arch, which have been associated with an increased risk of re-CoA in previous studies [32,53]. Young age of <15 days and low preoperative weight of ≤2.5 kg at neonatal CoA repair were not risk factors for re-CoA in our study, in contrast to a previous study [43].

Aortic arch geometry in relation to re-CoA

Previous studies have suggested an association between a postoperative crenel or gothic arch shape and re-CoA [48,54]. In our study, all infants with re-CoA had a crenel arch configuration, whereas the two with a gothic arch did not develop re-CoA.

Another interesting finding, not previously reported, was that infants, who developed re-CoA had smaller angles between the ascending aorta and the brachiocephalic artery and between the proximal aortic arch and the left common carotid artery. Intuitively, proximal branching vessels more aligned with the distal ascending aorta, especially in a crenel arch with a smaller transverse segment, as

seen in most patients with end-to-end or extended end-to-end anastomosis, could result in abnormal flow streaming with consequent altered flow and re-CoA. However, this could not be demonstrated in our study. Calibre mismatch with a larger ascending aorta and brachiocephalic artery and a smaller transverse aortic arch may be of greater importance than arch geometry for changes in flow [135] and in the occurrence of re-CoA, as suggested by our results.

Changes in flow pattern in the distal aortic arch in relation to re-CoA

Infants, who developed re-CoA had more left-handed systolic helical and right-handed diastolic helical flow, as well as less vortical flow than those who did not develop re-CoA. An MRI study conducted more than 10 years after CoA repair showed no difference in overall helicity, but an increase in local helicity and vorticity in different segments of the aorta compared to healthy controls [136]. In contrast to our study, the majority of these patients had undergone resection with end-to-end anastomosis, and none had re-CoA [136]. Importantly, these changes were not limited to the specific region of repair [136]. In our study, we did not examine the entire aortic arch. Instead, we focused on the distal transverse arch down to the proximal descending aorta including the isthmic region of the aortic arch, where re-CoA usually occurs. In addition, our cohort included much younger patients who underwent MRI within days of neonatal CoA repair, and flow patterns were not compared with healthy controls.

All of this could explain the differences in findings compared to our study.

Clinical data prior to discharge and their relation to re-CoA

Previous studies have identified higher early, pre-discharge isthmic peak flow velocity and systolic pressure gradient between arm and leg as risk factors for re-CoA [52,53]. In our study, only peak flow velocity was associated with re-CoA. Some inherent difficulties in reliably measuring blood pressure in infants may be a possible explanation for the lack of differences in pre-discharge blood pressure gradients.

Conclusions

The four papers included in this thesis add to the current knowledge of prenatal diagnosis (Papers I and III) and neonatal pre- and postoperative risk stratification (Papers II and IV) in patients with severe left heart obstructions. These new insights may aid to improve neonatal care and outcome.

Paper I

In this study, we demonstrated that CoA can be predicted with high accuracy in late gestation using the CSAI or the I/D3VTxMV/TV. The I/D3VTxMV/TV may be superior to the CSAI, because it captures the disproportion between the ventricles and the isthmus and arterial duct, without the need for the sagittal aortic arch view, which can be difficult to obtain in late gestation.

Ratios were more reliable predictors of CoA than Z-scores. Also, there were significant differences between Z-score datasets for the same measurements, which the operator needs to be aware of in order to make an accurate diagnosis.

Paper II

In this study, we showed that both the anatomic HLHS subtype AA-MS and the globular left ventricular phenotype were associated with morbidity and mortality. Patients with these morphological variants who underwent Norwood stage I palliation using a BTs had an even worse outcome. Awareness of these factors may help to select the optimal neonatal surgical approach and plan for optimal short- and long term follow-up.

Paper III

The use of fetal CMR-derived flow measurements in the DAo and UV could not aid to discriminate between fetuses who would or would not require neonatal intervention for left heart obstructions. However, it was possible to identify those with severely impaired flow across the left side of the heart, including fetuses with retrograde systolic isthmic flow in HLHS, cAS or suspected CoA. This information may be particularly useful in late gestation, when acoustic windows are poor.

Paper IV

In this study, we found that MRI-based 3D aortic arch geometry and 4D flow pattern, including helicity and vorticity, can be assessed in neonates after CoA repair and may be a useful method to further investigate the relationship between the complex aortic arch geometry and flow after neonatal CoA repair. Further understanding of the aortic arch geometry and flow in the formation of re-CoA may be important to improve outcomes after neonatal CoA repair.

Future Perspectives

Based on the findings of this thesis, future research could include:

1. A large, multicentre prospective fetal echocardiography study to validate the CSAI and I/D3VTxMV/TV in the fetal diagnosis of CoA.
2. Large multicentre prospective fetal echocardiography and CMR studies of left heart obstructions and of other CHDs to further assess the additive role of the MRI technique and to validate newer fetal echocardiographic techniques (e.g. 3D or strain) in order to improve fetal diagnosis and predict neonatal outcome.
3. Multicentre studies to generate reliable fetal echocardiographic Z-scores.
4. A prospective, multicentre study in patients with HLHS to further assess the impact of a globular left ventricle on systemic right ventricular function and outcome and to determine differences in these two in patients with a globular LV in the presence or absence of the anatomic subtype AA-MS.
5. A large national prospective MRI study to assess the influence of aortic arch geometry and flow on re-CoA formation and systemic hypertension.

Acknowledgements

Petru Liuba, my main research supervisor and guru. Creative, bursting with clever ideas, incredibly social and able to gather a large number of followers (PhD students) around him. He has at least 30 juggling balls in the air at any one time, ranging from clinical work, a multitude of research projects, national and international collaborations, lectures to give, catheter interventions abroad, but also private matters such as visiting relatives, or dealing with discharged or broken cars or robotic lawnmowers. It seems that your day is longer than 24 hours. The only time you rest is every Sunday for 2 hours in order to reflect on the meaning of life. To cope with this multitude of daily tasks, one needs to have a certain mind set, one of which is to be a time optimist. With this attitude, nothing is urgent and we always have "plenty of time" until 2 days before the deadline. But then everything changes: the stress is there, the work has to be done and, like a miracle, we always managed to do it just minutes before the deadline. Time and time again I have been surprised that we have been successful with this strategy, but we have been...always. Thank you, Petru, for your expertise, creativity, social skills, time optimism, sense of humour and unorthodox supervision!

Katarina Hanséus, head of department and one of my co-supervisors: a haven of calm and peace in a sea of stressful multitasking and frothing emotions, with a big heart for her employees. Advice (in your own words, “the sermon”) on professional, research and personal matters was offered here and there and gratefully accepted. Thank you for your listening ear and good advice! And thank you for giving me time and support for my doctoral studies.

Erik Hedström, one of the few fetal MRI experts worldwide and one of my co-supervisors: thank you for introducing me to the mysteries of fetal cardiac MRI, a new and fascinating technique, and for giving me the opportunity to give talks on it at international conferences.

Constance Weismann, friend, compatriot and one of my co-supervisors: a great mind, clever to think, precise to write and always direct in her feedback. Thank you for your wise, prompt and reliable feedback!

Pia Sjöberg, MRI expert and one of my co-supervisors. Thank you for your straightforward way of giving feedback on research matters as well as on the quality of the art films we watched together.

Johannes Töger, Einar Heiberg & Lea Christierson: thank you for your easy and professional 24/7 availability in order to give me new insights into the secrets of MRI flow, 3D volume- and 3D angle calculations, all on top of teaching courses, childcare and other family matters you had to deal with at the same time. Zoom meetings on Sundays after 8 pm: no problem!

Marjolein Piek & Daniel Ryd: thank you for your great cooperation, accessibility and excellent performance of fetal MRI scans. This has enabled progress to be made in the use of fetal MRI in clinical and research settings. And of course, thank you for your great sense of humour, which made working together a pleasure.

Co-authors in Lund, Gothenburg, Stockholm and Umeå: Jens Johansson Ramgren, Phan-Kiet Tran, Mats Mellander, Jan Sunnegårdh, Mats Synnergren, Gunnar Sjöberg, Magnus Dalén, Annika Rydberg for a fantastic national collaboration with assistance in accessing data and images, as well as valuable input that helped improve the HLHS manuscript.

Eva Nordin and Elin Friberg, what would Lund's research group be without your dedication? You make an important contribution to taming the chaos created by PhD students and supervisors. When should we apply for which funding? When is the next PhD student meeting? Where can I find the ethics application form for study A? What is the funding number? Can you help me book the room for my disputation? We need an MRI scan for patient B. Can it be done within the next 2 days? But you are so much more than that! It is always nice to have a chat in the corridor and talk about research and private matters. And we have often laughed together (for example about the train prank you played on me, Elin). So good to have you in our research team!

PhD Group: an inspiring group of peers with whom I have been through thick and thin. Our activities together (those long Wednesday afternoons) ranged from journal clubs, to short summaries of our projects, to presentations of completed or forthcoming studies, to test presentations/mock exams for those who were about to present at international conferences, or who had their midterm control or dissertations to complete. It has been a pleasure to be part of this community. Keep up the good work! And you won't get rid of me so easily. I will be happy to attend the next meetings (if I am allowed to).

Michal Odermarsky, one of the most generous and helpful colleagues you could ever have. You knew all the secrets of the Stone Age statistical programme Statview, and you also knew how to dress properly for the Oktoberfest (no one can beat your Tyrolean hat and lederhosen).

Fetal team in Malmö and Lund including midwifes, specialized obstetricians, liaison nurses and fetal cardiologists: without your expertise, timely detection and correct prenatal diagnosis of CHDs wouldn´t be possible, which would probably result in a much worse start in life for our patients! The excellent detection rates in Lund and Malmö are something to celebrate, and the launch of "Fosterhjärtats År" is an important step towards improving detection rates nationwide. Thank you for your great work, collaboration and support of our fetal research projects, which have enabled us to gain important knowledge that may be applicable to clinical practice in the future.

Colleagues in pediatric cardiology, pediatric cardiac surgery and pediatric intensive care: thank you for working so hard to improve the lives of children with cardiac conditions and their families. Your expertise and dedication are indispensable. As I leave my desk, I look forward to being back in clinical practice and working with you again! Our work matters!

Dear friends: it is so good to have you in my life. However, between clinical work, research, administration and family, there has not always been as much time as I would have liked to spend together. With the completion of my PhD, I promise to make more time for you!

To **my parents and sister:** thank you for your loving and unconditional support and good advice, both on a personal and professional level.

Tillmann, Josephine, Jonathan and Hannah:
Both great loves and tornados of my non-professional life: I love you!
Tillmann: thank you so much for being a good father and taking good care of our children, especially when I needed it most! I know it hasn't always been easy!
Josephine, Jonathan & Hannah: thank you for enduring the frequent (nightly) sight of a tired mum behind her laptop. I know you didn't like it and have since vowed never to do anything that "boring" yourselves. And thank you for all the alternative career suggestions you gave me, such as blogger/influencer, hairdresser or vegetarian restaurant owner. It's always good to have a plan B.

Finally, thank you to myself for writing a thesis for the second (and last?) time in my career. Colleagues and friends were sometimes horrified at the idea of doing it twice. To be honest, I love learning and discovering new things, especially those that initially seem daunting, overwhelming and unattainable. Research, a future vocation?

This thesis was supported with grants from the Swedish Heart-Lung Foundation (HLF), the Swedish Children´s Heart Association (Hjärtebarnsfonden), the Swedish Governmental Funding of Clinical Research (ALF), the Swedish Research Council (Vetenskapsrådet), Region Skåne and Skåne University Hospital Lund.

References

1. Rosenthal E. Coarctation of the aorta from fetus to adult: curable condition or life long disease process? *Heart.* Nov 2005;91(11):1495-1502.

2. Lannering K, Kazamia K, Bergman G, et al. Screening for Critical Congenital Heart Defects in Sweden. *Pediatrics.* Oct 1 2023;152(4).

3. Holland BJ, Myers JA, Woods CR, Jr. Prenatal diagnosis of critical congenital heart disease reduces risk of death from cardiovascular compromise prior to planned neonatal cardiac surgery: a meta-analysis. *Ultrasound Obstet Gynecol.* Jun 2015;45(6):631-638.

4. Evers PD, Ranade D, Lewin M, Arya B. Diagnostic Approach in Fetal Coarctation of the Aorta: A Cost-Utility Analysis. *J Am Soc Echocardiogr.* Jun 2017;30(6):589-594.

5. Lytzen R, Vejlstrup N, Bjerre J, et al. Live-Born Major Congenital Heart Disease in Denmark: Incidence, Detection Rate, and Termination of Pregnancy Rate From 1996 to 2013. *JAMA Cardiol.* Sep 1 2018;3(9):829-837.

6. Carvalho JS, Mavrides E, Shinebourne EA, Campbell S, Thilaganathan B. Improving the effectiveness of routine prenatal screening for major congenital heart defects. *Heart.* Oct 2002;88(4):387-391.

7. Anuwutnavin S, Satou G, Chang RK, DeVore GR, Abuel A, Sklansky M. Prenatal Sonographic Predictors of Neonatal Coarctation of the Aorta. *J Ultrasound Med.* Nov 2016;35(11):2353-2364.

8. Beattie M, Peyvandi S, Ganesan S, Moon-Grady A. Toward Improving the Fetal Diagnosis of Coarctation of the Aorta. *Pediatr Cardiol.* Feb 2017;38(2):344-352.

9. Gomez-Montes E, Herraiz I, Gomez-Arriaga PI, Escribano D, Mendoza A, Galindo A. Gestational age-specific scoring systems for the prediction of coarctation of the aorta. *Prenat Diagn.* Dec 2014;34(12):1198-1206.

10. van Nisselrooij AEL, Rozendaal L, Linskens IH, et al. Postnatal outcome of fetal isolated ventricular size disproportion in the absence of aortic coarctation. *Ultrasound Obstet Gynecol.* Nov 2018;52(5):593-598.

11. Tuo G, Paladini D, Marasini L, et al. Fetal aortic coarctation: A combination of third-trimester echocardiographic parameters to improve the prediction of postnatal outcome. *Front Pediatr.* 2022;10:866994.

12. Hornberger LK, Sahn DJ, Kleinman CS, Copel J, Silverman NH. Antenatal diagnosis of coarctation of the aorta: a multicenter experience. *J Am Coll Cardiol.* Feb 1994;23(2):417-423.

13. Quartermain MD, Cohen MS, Dominguez TE, Tian Z, Donaghue DD, Rychik J. Left ventricle to right ventricle size discrepancy in the fetus: the presence of

critical congenital heart disease can be reliably predicted. *J Am Soc Echocardiogr.* Nov 2009;22(11):1296-1301.

14. Slodki M, Rychik J, Moszura T, Janiak K, Respondek-Liberska M. Measurement of the great vessels in the mediastinum could help distinguish true from false-positive coarctation of the aorta in the third trimester. *J Ultrasound Med.* Oct 2009;28(10):1313-1317.

15. Matsui H, Mellander M, Roughton M, Jicinska H, Gardiner HM. Morphological and physiological predictors of fetal aortic coarctation. *Circulation.* Oct 28 2008;118(18):1793-1801.

16. Arya B, Bhat A, Vernon M, Conwell J, Lewin M. Utility of novel fetal echocardiographic morphometric measures of the aortic arch in the diagnosis of neonatal coarctation of the aorta. *Prenat Diagn.* Feb 2016;36(2):127-134.

17. Familiari A, Morlando M, Khalil A, et al. Risk Factors for Coarctation of the Aorta on Prenatal Ultrasound: A Systematic Review and Meta-Analysis. *Circulation.* Feb 21 2017;135(8):772-785.

18. Toole BJ, Schlosser B, McCracken CE, Stauffer N, Border WL, Sachdeva R. Importance of Relationship between Ductus and Isthmus in Fetal Diagnosis of Coarctation of Aorta. *Echocardiography.* May 2016;33(5):771-777.

19. DeVore GR, Cuneo B, Klas B, Satou G, Sklansky M. Comprehensive Evaluation of Fetal Cardiac Ventricular Widths and Ratios Using a 24-Segment Speckle Tracking Technique. *J Ultrasound Med.* Apr 2019;38(4):1039-1047.

20. Chen Z, Zhou Y, Wang J, Liu X, Ge S, He Y. Modeling of coarctation of aorta in human fetuses using 3D/4D fetal echocardiography and computational fluid dynamics. *Echocardiography.* Dec 2017;34(12):1858-1866.

21. Lloyd DFA, van Poppel MPM, Pushparajah K, et al. Analysis of 3-Dimensional Arch Anatomy, Vascular Flow, and Postnatal Outcome in Cases of Suspected Coarctation of the Aorta Using Fetal Cardiac Magnetic Resonance Imaging. *Circ Cardiovasc Imaging.* Jul 2021;14(7):e012411.

22. Weber RW, Ayala-Arnez R, Atiyah M, et al. Foetal echocardiographic assessment of borderline small left ventricles can predict the need for postnatal intervention. *Cardiol Young.* Feb 2013;23(1):99-107.

23. Venardos A, Colquitt J, Morris SA. Fetal growth of left-sided structures and postnatal surgical outcome in borderline left heart varies by cardiac phenotype. *Ultrasound Obstet Gynecol.* May 2022;59(5):642-650.

24. Rudolph AM, Heymann MA, Spitznas U. Hemodynamic considerations in the development of narrowing of the aorta. *Am J Cardiol.* Oct 1972;30(5):514-525.

25. Hutchins GM. Coarctation of the aorta explained as a branch-point of the ductus arteriosus. *Am J Pathol.* May 1971;63(2):203-214.

26. Doshi AR, Chikkabyrappa S. Coarctation of Aorta in Children. *Cureus.* Dec 5 2018;10(12):e3690.

27. Ryd D, Sun L, Steding-Ehrenborg K, et al. Quantification of blood flow in the fetus with cardiovascular magnetic resonance imaging using Doppler ultrasound gating: validation against metric optimized gating. *J Cardiovasc Magn Reson.* Nov 28 2019;21(1):74.

28. Dodge-Khatami A, Ott S, Di Bernardo S, Berger F. Carotid-subclavian artery index: new echocardiographic index to detect coarctation in neonates and infants. *Ann Thorac Surg.* Nov 2005;80(5):1652-1657.
29. Bhatt AB, Lantin-Hermoso MR, Daniels CJ, et al. Isolated Coarctation of the Aorta: Current Concepts and Perspectives. *Front Cardiovasc Med.* 2022;9:817866.
30. Amato JJ, Rheinlander HF, Cleveland RJ. A method of enlarging the distal transverse arch in infants with hypoplasia and coarctation of the aorta. *Ann Thorac Surg.* Mar 1977;23(3):261-263.
31. Mery CM, Guzman-Pruneda FA, Carberry KE, et al. Aortic arch advancement for aortic coarctation and hypoplastic aortic arch in neonates and infants. *Ann Thorac Surg.* Aug 2014;98(2):625-633; discussion 633.
32. Rakhra SS, Lee M, Iyengar AJ, et al. Poor outcomes after surgery for coarctation repair with hypoplastic arch warrants more extensive initial surgery and close long-term follow-up. *Interact Cardiovasc Thorac Surg.* Jan 2013;16(1):31-36.
33. Gray WH, Wells WJ, Starnes VA, Kumar SR. Arch Augmentation via Median Sternotomy for Coarctation of Aorta With Proximal Arch Hypoplasia. *Ann Thorac Surg.* Oct 2018;106(4):1214-1219.
34. Farag ES, Kluin J, de Heer F, et al. Aortic coarctation repair through left thoracotomy: results in the modern era. *Eur J Cardiothorac Surg.* Feb 1 2019;55(2):331-337.
35. Vigneswaran TV, Sinha MD, Valverde I, Simpson JM, Charakida M. Hypertension in Coarctation of the Aorta: Challenges in Diagnosis in Children. *Pediatr Cardiol.* Jan 2018;39(1):1-10.
36. de Divitiis M, Pilla C, Kattenhorn M, et al. Vascular dysfunction after repair of coarctation of the aorta: impact of early surgery. *Circulation.* Sep 18 2001;104(12 Suppl 1):I165-170.
37. Vogt M, Kuhn A, Baumgartner D, et al. Impaired elastic properties of the ascending aorta in newborns before and early after successful coarctation repair: proof of a systemic vascular disease of the prestenotic arteries? *Circulation.* Jun 21 2005;111(24):3269-3273.
38. Bailie MD, Donoso VS, Gonzalez NC. Role of the renin-angiotensin system in hypertension after coarctation of the aorta. *J Lab Clin Med.* Oct 1984;104(4):553-562.
39. Polson JW, McCallion N, Waki H, et al. Evidence for cardiovascular autonomic dysfunction in neonates with coarctation of the aorta. *Circulation.* Jun 20 2006;113(24):2844-2850.
40. Ou P, Bonnet D, Auriacombe L, et al. Late systemic hypertension and aortic arch geometry after successful repair of coarctation of the aorta. *Eur Heart J.* Oct 2004;25(20):1853-1859.
41. Hager A, Schreiber C, Nutzl S, Hess J. Mortality and restenosis rate of surgical coarctation repair in infancy: a study of 191 patients. *Cardiology.* 2009;112(1):36-41.

42. Minotti C, Scioni M, Castaldi B, et al. Effectiveness of Repair of Aortic Coarctation in Neonates: A Long-Term experience. *Pediatr Cardiol.* Jan 2022;43(1):17-26.
43. Lehnert A, Villemain O, Gaudin R, Meot M, Raisky O, Bonnet D. Risk factors of mortality and recoarctation after coarctation repair in infancy. *Interact Cardiovasc Thorac Surg.* Sep 1 2019;29(3):469-475.
44. Wright GE, Nowak CA, Goldberg CS, Ohye RG, Bove EL, Rocchini AP. Extended resection and end-to-end anastomosis for aortic coarctation in infants: results of a tailored surgical approach. *Ann Thorac Surg.* Oct 2005;80(4):1453-1459.
45. Kaushal S, Backer CL, Patel JN, et al. Coarctation of the aorta: midterm outcomes of resection with extended end-to-end anastomosis. *Ann Thorac Surg.* Dec 2009;88(6):1932-1938.
46. Mery CM, Guzman-Pruneda FA, Trost JG, Jr., et al. Contemporary Results of Aortic Coarctation Repair Through Left Thoracotomy. *Ann Thorac Surg.* Sep 2015;100(3):1039-1046.
47. Lee H, Yang JH, Jun TG, et al. Augmentation of the Lesser Curvature With an Autologous Vascular Patch in Complex Aortic Coarctation and Interruption. *Ann Thorac Surg.* Jun 2016;101(6):2309-2314.
48. Seo DM, Park J, Goo HW, Kim YH, Ko JK, Jhang WK. Surgical modification for preventing a gothic arch after aortic arch repair without the use of foreign material. *Interact Cardiovasc Thorac Surg.* Apr 2015;20(4):504-509.
49. Adamson G, Karamlou T, Moore P, Natal-Hernandez L, Tabbutt S, Peyvandi S. Coarctation Index Predicts Recurrent Aortic Arch Obstruction Following Surgical Repair of Coarctation of the Aorta in Infants. *Pediatr Cardiol.* Aug 2017;38(6):1241-1246.
50. McElhinney DB, Yang SG, Hogarty AN, et al. Recurrent arch obstruction after repair of isolated coarctation of the aorta in neonates and young infants: is low weight a risk factor? *J Thorac Cardiovasc Surg.* Nov 2001;122(5):883-890.
51. Burch PT, Cowley CG, Holubkov R, et al. Coarctation repair in neonates and young infants: is small size or low weight still a risk factor? *J Thorac Cardiovasc Surg.* Sep 2009;138(3):547-552.
52. Truong DT, Tani LY, Minich LL, Burch PT, Bardsley TR, Menon SC. Factors associated with recoarctation after surgical repair of coarctation of the aorta by way of thoracotomy in young infants. *Pediatr Cardiol.* Jan 2014;35(1):164-170.
53. Kumar TK, Zurakowski D, Sharma R, Saini S, Jonas RA. Prediction of recurrent coarctation by early postoperative blood pressure gradient. *J Thorac Cardiovasc Surg.* Nov 2011;142(5):1130-1136, 1136 e1131.
54. Chiu HH, Chiu SN, Hu FC, et al. Late cardiovascular complications after surgical or balloon angioplasty of coarctation of aorta in an Asian cohort. *Am J Cardiol.* Oct 15 2009;104(8):1139-1144.
55. Kritzmire SM, Cossu AE. Hypoplastic Left Heart Syndrome. *StatPearls*. Treasure Island (FL) ineligible companies. Disclosure: Anne Cossu declares no relevant financial relationships with ineligible companies.2023.

56. Yabrodi M, Mastropietro CW. Hypoplastic left heart syndrome: from comfort care to long-term survival. *Pediatr Res.* Jan 2017;81(1-2):142-149.
57. Norwood WI, Kirklin JK, Sanders SP. Hypoplastic left heart syndrome: experience with palliative surgery. *Am J Cardiol.* Jan 1980;45(1):87-91.
58. Mascio CE, Irons ML, Ittenbach RF, et al. Thirty years and 1663 consecutive Norwood procedures: Has survival plateaued? *J Thorac Cardiovasc Surg.* Jul 2019;158(1):220-229.
59. Sano S, Ishino K, Kawada M, et al. Right ventricle-pulmonary artery shunt in first-stage palliation of hypoplastic left heart syndrome. *J Thorac Cardiovasc Surg.* Aug 2003;126(2):504-509; discussion 509-510.
60. Ohye RG, Sleeper LA, Mahony L, et al. Comparison of shunt types in the Norwood procedure for single-ventricle lesions. *N Engl J Med.* May 27 2010;362(21):1980-1992.
61. Tworetzky W, McElhinney DB, Reddy VM, Brook MM, Hanley FL, Silverman NH. Improved surgical outcome after fetal diagnosis of hypoplastic left heart syndrome. *Circulation.* Mar 6 2001;103(9):1269-1273.
62. Metcalf MK, Rychik J. Outcomes in Hypoplastic Left Heart Syndrome. *Pediatr Clin North Am.* Oct 2020;67(5):945-962.
63. Rychik J, Szwast A, Natarajan S, et al. Perinatal and early surgical outcome for the fetus with hypoplastic left heart syndrome: a 5-year single institutional experience. *Ultrasound Obstet Gynecol.* Oct 2010;36(4):465-470.
64. Glatz JA, Tabbutt S, Gaynor JW, et al. Hypoplastic left heart syndrome with atrial level restriction in the era of prenatal diagnosis. *Ann Thorac Surg.* Nov 2007;84(5):1633-1638.
65. Saul D, Degenhardt K, Iyoob SD, et al. Hypoplastic left heart syndrome and the nutmeg lung pattern in utero: a cause and effect relationship or prognostic indicator? *Pediatr Radiol.* Apr 2016;46(4):483-489.
66. Tabbutt S, Ghanayem N, Ravishankar C, et al. Risk factors for hospital morbidity and mortality after the Norwood procedure: A report from the Pediatric Heart Network Single Ventricle Reconstruction trial. *J Thorac Cardiovasc Surg.* Oct 2012;144(4):882-895.
67. Hehir DA, Dominguez TE, Ballweg JA, et al. Risk factors for interstage death after stage 1 reconstruction of hypoplastic left heart syndrome and variants. *J Thorac Cardiovasc Surg.* Jul 2008;136(1):94-99, 99 e91-93.
68. Iyengar AJ, Winlaw DS, Galati JC, et al. Trends in Fontan surgery and risk factors for early adverse outcomes after Fontan surgery: the Australia and New Zealand Fontan Registry experience. *J Thorac Cardiovasc Surg.* Aug 2014;148(2):566-575.
69. Rychik J, Atz AM, Celermajer DS, et al. Evaluation and Management of the Child and Adult With Fontan Circulation: A Scientific Statement From the American Heart Association. *Circulation.* Aug 6 2019;140(6):e234-e284.
70. Calderon J, Newburger JW, Rollins CK. Neurodevelopmental and Mental Health Outcomes in Patients With Fontan Circulation: A State-of-the-Art Review. *Front Pediatr.* 2022;10:826349.

71. Tchervenkov CI, Jacobs JP, Weinberg PM, et al. The nomenclature, definition and classification of hypoplastic left heart syndrome. *Cardiol Young.* Aug 2006;16(4):339-368.
72. Jonas RA, Hansen DD, Cook N, Wessel D. Anatomic subtype and survival after reconstructive operation for hypoplastic left heart syndrome. *J Thorac Cardiovasc Surg.* Apr 1994;107(4):1121-1127; discussion 1127-1128.
73. Forbess JM, Cook N, Roth SJ, Serraf A, Mayer JE, Jr., Jonas RA. Ten-year institutional experience with palliative surgery for hypoplastic left heart syndrome. Risk factors related to stage I mortality. *Circulation.* Nov 1 1995;92(9 Suppl):II262-266.
74. Jacobs ML. Aortic reconstruction in hypoplastic left heart syndrome-A reappraisal. *J Thorac Cardiovasc Surg.* Nov 2000;120(5):872-874.
75. Glatz JA, Fedderly RT, Ghanayem NS, Tweddell JS. Impact of mitral stenosis and aortic atresia on survival in hypoplastic left heart syndrome. *Ann Thorac Surg.* Jun 2008;85(6):2057-2062.
76. Furck AK, Uebing A, Hansen JH, et al. Outcome of the Norwood operation in patients with hypoplastic left heart syndrome: a 12-year single-center survey. *J Thorac Cardiovasc Surg.* Feb 2010;139(2):359-365.
77. Shuhaiber J, Morgan B, Gottliebson W. Survival outcomes following norwood procedure for hypoplastic left heart. *Pediatr Cardiol.* Jan 2015;36(1):57-63.
78. Crucean A, Alqahtani A, Barron DJ, et al. Re-evaluation of hypoplastic left heart syndrome from a developmental and morphological perspective. *Orphanet J Rare Dis.* Aug 10 2017;12(1):138.
79. Grossfeld P, Nie S, Lin L, Wang L, Anderson RH. Hypoplastic Left Heart Syndrome: A New Paradigm for an Old Disease? *J Cardiovasc Dev Dis.* Feb 23 2019;6(1).
80. Fricke K, Mellander M, Hanseus K, et al. Impact of Left Ventricular Morphology on Adverse Outcomes Following Stage 1 Palliation for Hypoplastic Left Heart Syndrome: 20 Years of National Data From Sweden. *J Am Heart Assoc.* Apr 5 2022;11(7):e022929.
81. Son JS, James A, Fan CS, et al. Prognostic Value of Serial Echocardiography in Hypoplastic Left Heart Syndrome. *Circ Cardiovasc Imaging.* Jul 2018;11(7):e006983.
82. Wang AP, Kelle AM, Hyun M, et al. Negative Impact of the Left Ventricular Remnant Morphology on Systemic Right Ventricular Myocardial Deformation in Hypoplastic Left Heart Syndrome. *Pediatr Cardiol.* Feb 2021;42(2):278-288.
83. Forsha D, Li L, Joseph N, Kutty S, Friedberg MK. Association of left ventricular size with regional right ventricular mechanics in Hypoplastic Left Heart Syndrome. *Int J Cardiol.* Jan 1 2020;298:66-71.
84. Walsh MA, McCrindle BW, Dipchand A, et al. Left ventricular morphology influences mortality after the Norwood operation. *Heart.* Aug 2009;95(15):1238-1244.
85. Hamzah M, Othman HF, Elsamny E, Agarwal H, Aly H. Clinical Outcomes and Risk Factors for In-Hospital Mortality in Neonates with Hypoplastic Left Heart Syndrome. *Pediatr Cardiol.* Apr 2020;41(4):781-788.

86. Ono M, Kido T, Wallner M, et al. Preoperative risk factors influencing inter-stage mortality after the Norwood procedure. *Interact Cardiovasc Thorac Surg.* Jul 26 2021;33(2):218-226.
87. Gabbay-Benziv R, Turan OM, Harman C, Turan S. Nomograms for Fetal Cardiac Ventricular Width and Right-to-Left Ventricular Ratio. *J Ultrasound Med.* Nov 2015;34(11):2049-2055.
88. Krishnan A, Pike JI, McCarter R, et al. Predictive Models for Normal Fetal Cardiac Structures. *J Am Soc Echocardiogr.* Dec 2016;29(12):1197-1206.
89. Pasquini L, Mellander M, Seale A, et al. Z-scores of the fetal aortic isthmus and duct: an aid to assessing arch hypoplasia. *Ultrasound Obstet Gynecol.* Jun 2007;29(6):628-633.
90. Schneider C, McCrindle BW, Carvalho JS, Hornberger LK, McCarthy KP, Daubeney PE. Development of Z-scores for fetal cardiac dimensions from echocardiography. *Ultrasound Obstet Gynecol.* Nov 2005;26(6):599-605.
91. Graziano JN, Heidelberger KP, Ensing GJ, Gomez CA, Ludomirsky A. The influence of a restrictive atrial septal defect on pulmonary vascular morphology in patients with hypoplastic left heart syndrome. *Pediatr Cardiol.* Mar-Apr 2002;23(2):146-151.
92. Fricke K, Liuba P, Weismann CG. Fetal Echocardiographic Dimension Indices: Important Predictors of Postnatal Coarctation. *Pediatr Cardiol.* Mar 2021;42(3):517-525.
93. Divanovic A, Hor K, Cnota J, Hirsch R, Kinsel-Ziter M, Michelfelder E. Prediction and perinatal management of severely restrictive atrial septum in fetuses with critical left heart obstruction: clinical experience using pulmonary venous Doppler analysis. *J Thorac Cardiovasc Surg.* Apr 2011;141(4):988-994.
94. Kording F, Yamamura J, de Sousa MT, et al. Dynamic fetal cardiovascular magnetic resonance imaging using Doppler ultrasound gating. *J Cardiovasc Magn Reson.* Mar 12 2018;20(1):17.
95. Ryd D, Nilsson A, Heiberg E, Hedstrom E. Automatic Segmentation of the Fetus in 3D Magnetic Resonance Images Using Deep Learning: Accurate and Fast Fetal Volume Quantification for Clinical Use. *Pediatr Cardiol.* Nov 5 2022.
96. Heiberg E, Sjogren J, Ugander M, Carlsson M, Engblom H, Arheden H. Design and validation of Segment--freely available software for cardiovascular image analysis. *BMC Med Imaging.* Jan 11 2010;10:1.
97. Koo TK, Li MY. A Guideline of Selecting and Reporting Intraclass Correlation Coefficients for Reliability Research. *J Chiropr Med.* Jun 2016;15(2):155-163.
98. Sjoberg P, Hedstrom E, Fricke K, et al. Comparison of 2D and 4D Flow MRI in Neonates Without General Anesthesia. *J Magn Reson Imaging.* Jan 2023;57(1):71-82.
99. Heiberg E, Ebbers T, Wigström L, Karlsson M. Three-dimensional flow characterization using vector pattern matching. *Ieee T Vis Comput Gr.* Jul-Sep 2003;9(3):313-319.
100. Fricke K, Ryd D, Weismann CG, Hanseus K, Hedstrom E, Liuba P. Fetal cardiac magnetic resonance imaging of the descending aorta in suspected left-sided cardiac obstructions. *Front Cardiovasc Med.* 2023;10:1285391.

101. Sivanandam S, Nyholm J, Wey A, Bass JL. Right Ventricular Enlargement In Utero: Is It Coarctation? *Pediatr Cardiol.* Oct 2015;36(7):1376-1381.
102. Patel C, Weeks B, Copel J, et al. Fetal Echocardiographic Measures to Improve the Prenatal Diagnosis of Coarctation of the Aorta. *Pediatr Cardiol.* Dec 13 2018.
103. Morgan CT, Mueller B, Thakur V, et al. Improving Prenatal Diagnosis of Coarctation of the Aorta. *Can J Cardiol.* Apr 2019;35(4):453-461.
104. Siehr SL, Maeda K, Connolly AA, et al. Mitral Stenosis and Aortic Atresia--A Risk Factor for Mortality After the Modified Norwood Operation in Hypoplastic Left Heart Syndrome. *Ann Thorac Surg.* Jan 2016;101(1):162-167.
105. Vida VL, Bacha EA, Larrazabal A, et al. Surgical outcome for patients with the mitral stenosis-aortic atresia variant of hypoplastic left heart syndrome. *J Thorac Cardiovasc Surg.* Feb 2008;135(2):339-346.
106. Nathan M, Williamson AK, Mayer JE, Bacha EA, Juraszek AL. Mortality in hypoplastic left heart syndrome: review of 216 autopsy cases of aortic atresia with attention to coronary artery disease. *J Thorac Cardiovasc Surg.* Dec 2012;144(6):1301-1306.
107. Polimenakos AC, Sathanandam SK, Husayni TS, El Zein CF, Roberson DA, Ilbawi MN. Hypoplastic left heart syndrome and aortic atresia-mitral stenosis variant: role of myocardial protection strategy and impact of ventriculo-coronary connections after stage I palliation. *Pediatr Cardiol.* Oct 2011;32(7):929-939.
108. Cohen MS, Dagincourt N, Zak V, et al. The Impact of the Left Ventricle on Right Ventricular Function and Clinical Outcomes in Infants with Single-Right Ventricle Anomalies up to 14 Months of Age. *J Am Soc Echocardiogr.* Oct 2018;31(10):1151-1157.
109. Rosner A, Bharucha T, James A, Mertens L, Friedberg MK. Impact of Right Ventricular Geometry and Left Ventricular Hypertrophy on Right Ventricular Mechanics and Clinical Outcomes in Hypoplastic Left Heart Syndrome. *J Am Soc Echocardiogr.* Oct 2019;32(10):1350-1358.
110. Schlangen J, Fischer G, Steendijk P, et al. Does left ventricular size impact on intrinsic right ventricular function in hypoplastic left heart syndrome? *Int J Cardiol.* Aug 20 2013;167(4):1305-1310.
111. Loomba RS, Shah PH, Chandrasekar S. Short-term outcome comparison of Norwood procedures with right ventricle to pulmonary artery conduit versus modified Blalock-Taussig shunt: A meta-analysis. *Ann Pediatr Cardiol.* Jul 2011;4(2):145-149.
112. Azakie A, Martinez D, Sapru A, Fineman J, Teitel D, Karl TR. Impact of right ventricle to pulmonary artery conduit on outcome of the modified Norwood procedure. *Ann Thorac Surg.* May 2004;77(5):1727-1733.
113. Pizarro C, Malec E, Maher KO, et al. Right ventricle to pulmonary artery conduit improves outcome after stage I Norwood for hypoplastic left heart syndrome. *Circulation.* Sep 9 2003;108 Suppl 1:II155-160.
114. Riveros Perez E, Riveros R. Mathematical Analysis and Physical Profile of Blalock-Taussig Shunt and Sano Modification Procedure in Hypoplastic Left Heart Syndrome: Review of the Literature and Implications for the Anesthesiologist. *Semin Cardiothorac Vasc Anesth.* Jun 2017;21(2):152-164.

115. Wong J, Lamata P, Rathod RH, et al. Right ventricular morphology and function following stage I palliation with a modified Blalock-Taussig shunt versus a right ventricle-to-pulmonary artery conduit. *Eur J Cardiothorac Surg.* Jan 2017;51(1):50-57.
116. Fischbach J, Sinzobahamvya N, Haun C, et al. Interventions after Norwood procedure: comparison of Sano and modified Blalock-Taussig shunt. *Pediatr Cardiol.* Jan 2013;34(1):112-118.
117. Tweddell JS, Sleeper LA, Ohye RG, et al. Intermediate-term mortality and cardiac transplantation in infants with single-ventricle lesions: risk factors and their interaction with shunt type. *J Thorac Cardiovasc Surg.* Jul 2012;144(1):152-159.
118. Murtuza B, Stumper O, Wall D, et al. The effect of morphologic subtype on outcomes following the Sano-Norwood procedure. *Eur J Cardiothorac Surg.* Nov 2012;42(5):787-793.
119. Chen Z, Zhao H, Zhao Y, et al. Retrograde flow in aortic isthmus in normal and fetal heart disease by principal component analysis and computational fluid dynamics. *Echocardiography.* Feb 2022;39(2):166-177.
120. Chabaneix J, Fouron JC, Sosa-Olavarria A, et al. Profiling left and right ventricular proportional output during fetal life with a novel systolic index in the aortic isthmus. *Ultrasound Obstet Gynecol.* Aug 2014;44(2):176-181.
121. Al Nafisi B, van Amerom JF, Forsey J, et al. Fetal circulation in left-sided congenital heart disease measured by cardiovascular magnetic resonance: a case-control study. *J Cardiovasc Magn Reson.* Jul 27 2013;15(1):65.
122. Nawaytou HM, Peyvandi S, Brook MM, Silverman N, Moon-Grady AJ. Right Ventricular Systolic-to-Diastolic Time Index: Hypoplastic Left Heart Fetuses Differ Significantly from Normal Fetuses. *J Am Soc Echocardiogr.* Feb 2016;29(2):143-149.
123. Graupner O, Enzensberger C, Wieg L, et al. Evaluation of right ventricular function in fetal hypoplastic left heart syndrome by color tissue Doppler imaging. *Ultrasound Obstet Gynecol.* Jun 2016;47(6):732-738.
124. Kawamura H, Inamura N, Inoue Y, Kawazu Y, Kayatani F, Mitsuda N. Is retrograde blood flow of aortic isthmus useful for the prenatal screening of coarctation of the aorta by fetal color Doppler echocardiography? A preliminary study. *J Med Ultrason (2001).* Jul 2018;45(3):431-435.
125. Yamamoto Y, Khoo NS, Brooks PA, Savard W, Hirose A, Hornberger LK. Severe left heart obstruction with retrograde arch flow influences fetal cerebral and placental blood flow. *Ultrasound Obstet Gynecol.* Sep 2013;42(3):294-299.
126. Frydrychowicz A, Berger A, Munoz Del Rio A, et al. Interdependencies of aortic arch secondary flow patterns, geometry, and age analysed by 4-dimensional phase contrast magnetic resonance imaging at 3 Tesla. *Eur Radiol.* May 2012;22(5):1122-1130.
127. Geiger J, Markl M, Herzer L, et al. Aortic flow patterns in patients with Marfan syndrome assessed by flow-sensitive four-dimensional MRI. *J Magn Reson Imaging.* Mar 2012;35(3):594-600.

128. Schnell S, Smith DA, Barker AJ, et al. Altered aortic shape in bicuspid aortic valve relatives influences blood flow patterns. *Eur Heart J Cardiovasc Imaging.* Nov 2016;17(11):1239-1247.
129. Desai LP, Berhane H, Husain N, Robinson JD, Rigsby CK, Markl M. Altered 4-D magnetic resonance imaging flow characteristics in complex congenital aortic arch repair. *Pediatr Radiol.* Jan 2020;50(1):17-27.
130. Bruse JL, Khushnood A, McLeod K, et al. How successful is successful? Aortic arch shape after successful aortic coarctation repair correlates with left ventricular function. *J Thorac Cardiovasc Surg.* Feb 2017;153(2):418-427.
131. Ou P, Celermajer DS, Raisky O, et al. Angular (Gothic) aortic arch leads to enhanced systolic wave reflection, central aortic stiffness, and increased left ventricular mass late after aortic coarctation repair: evaluation with magnetic resonance flow mapping. *J Thorac Cardiovasc Surg.* Jan 2008;135(1):62-68.
132. Ou P, Celermajer DS, Mousseaux E, et al. Vascular remodeling after "successful" repair of coarctation: impact of aortic arch geometry. *J Am Coll Cardiol.* Feb 27 2007;49(8):883-890.
133. Szopos M, Poussineau N, Maday Y, et al. Computational modeling of blood flow in the aorta--insights into eccentric dilatation of the ascending aorta after surgery for coarctation. *J Thorac Cardiovasc Surg.* Oct 2014;148(4):1572-1582.
134. Qin J, Ouyang D, Yan T, et al. Using computed tomography angiography and computational fluid dynamics to study aortic coarctation in different arch morphologies. *Front Pediatr.* 2023;11:1131025.
135. Quail MA, Segers P, Steeden JA, Muthurangu V. The aorta after coarctation repair - effects of calibre and curvature on arterial haemodynamics. *J Cardiovasc Magn Reson.* Apr 11 2019;21(1):22.
136. Frydrychowicz A, Markl M, Hirtler D, et al. Aortic hemodynamics in patients with and without repair of aortic coarctation: in vivo analysis by 4D flow-sensitive magnetic resonance imaging. *Invest Radiol.* May 2011;46(5):317-325.
137. Dias MQ, Barros A, Leite-Moreira A, Miranda JO. Risk Factors for Recoarctation and Mortality in Infants Submitted to Aortic Coarctation Repair: A Systematic Review. *Pediatr Cardiol.* Mar 2020;41(3):561-575.
138. Miwa K, Iwai S, Tsumura S, et al. Influence of Bovine Arch Anatomy on Surgical Outcomes of Coarctation of the Aorta. *Pediatr Cardiol.* Apr 2023;44(4):933-939.

Printed by Media-Tryck, Lund 2024 NORDIC SWAN ECOLABEL 3041 0903

About the author

Katrin Fricke is a consultant in pediatric and fetal cardiology at the Children's Heart Centre, Skåne University Hospital, Lund, Sweden.

She trained as a pediatrician and pediatric cardiologist in Germany and Sweden.

Katrin is particularly interested in cardiac imaging from fetal life to adolescence.

Her research projects focus on left heart anomalies.

LUND UNIVERSITY

FACULTY OF MEDICINE

Department of Experimental Medical Science

Lund University, Faculty of Medicine
Doctoral Dissertation Series 2024:23
ISBN 978-91-8021-516-9
ISSN 1652-8220